

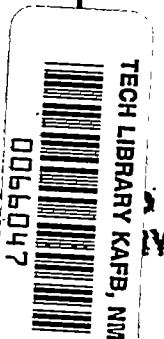
3543 E NACA TN 3254

NACA
TN
3254
c.1

NATIONAL ADVISORY COMMITTEE FOR AERONAUTICS

TECHNICAL NOTE 3254

LOAN COPY: RE
AFWL TECHNICAL
KIRTLAND AFB



DETERMINATION OF FLAME TEMPERATURES FROM 2000° TO 3000° K BY MICROWAVE ABSORPTION

By Perry W. Kuhns

Lewis Flight Propulsion Laboratory
Cleveland, Ohio



Washington
August 1954

AFM

TECHNICAL

AFM



NATIONAL ADVISORY COMMITTEE FOR AERONAUTICS

TECHNICAL NOTE 3254

DETERMINATION OF FLAME TEMPERATURES FROM 2000° TO 3000° K

2
GOT

BY MICROWAVE ABSORPTION

By Perry W. Kuhns

SUMMARY

Equations are derived for the measurement of flame temperatures from the attenuation of a microwave beam by temperature-induced free electrons from chemical elements introduced in the flame. Corrections are developed to account for the electron distribution in the flame. Procedure for obtaining the temperature from absorption is outlined.

CN-1

The free electron collision frequency and an effective ionization potential for four alkali elements were determined experimentally. The data were taken on a gas burner with a temperature range from 1900° to 2400° K. The effective ionization potential of sodium agrees with the spectral-line limit value. From these experimental ionization potentials and the experimental collision frequency, an accuracy of $\pm 60^{\circ}$ K in the temperature was obtained.

Fluctuating and average temperature data of a liquid propellant burner are presented primarily from 1.25-centimeter-wavelength microwave measurements in comparison with simultaneous two-color pyrometer and sound intensity measurements in the region from 2200° to 2900° K.

INTRODUCTION

Present experimental work on rockets and jet engines has shown the need for a method of measuring gas temperatures above 2000° K. Such a method to be practicable must be relatively insensitive to conditions outside the flame region of interest and to variations in gas flow. Because of the temperatures involved, such a method should not necessitate the presence of devices in the flame itself. Among such methods presently available are the sodium-line reversal, the "two-color" systems, the infrared and the ultraviolet radiation methods, and the method making use of temperature-dependent attenuation of radiation in the microwave region.

3109

The microwave attenuation method is dependent upon the absorption of electromagnetic waves by temperature-induced free electrons. The electron density, and thus the absorption power, is a function of the gas temperature. In most flames it is necessary to add an alkali salt of low ionization potential to supply sufficient free electrons.

Belcher and Sugden (refs. 1 and 2) used microwave absorption to determine the electron density in a study of the ionization of alkali salts in a flame. They concluded that deviations of electron density from the values calculated from Saha's equation could be explained by reactions producing alkali hydroxide and oxide compounds, and the production of electron acceptors. Rudlin (ref. 3) presented data showing the variation of attenuation with flame temperature in the region of 1900° to 2500° K and concluded that the attenuation was substantially independent of the halide component of the salt used.

The present work is concerned with (1) the determination of the collision frequency of free electrons in a flame, (2) the estimation of the effect of nonequilibrium and flame chemistry upon the effective ionization potential of the alkali element, (3) the extension of the idealized infinite-sheet formula to the case of attenuation of a microwave beam by a finite cylindrical flame, (4) the estimation of sensitivity of the attenuation measurement to variations in flame parameters such as temperature, flame size, gas flow, and salt concentration, and (5) the applicability of an instrument for the measurement of average flame temperatures and of time-fluctuating flame temperatures.

Microwave attenuation readings were taken on a blast burner for two wavelengths at temperatures between 1900° and 2400° K in conjunction with sodium-line reversal temperature measurements, and on a liquid propellant burner at temperatures between 2200° and 2900° K in conjunction with sodium-line reversal or two-color pyrometer measurements. Measurements of flame-temperature fluctuations on the liquid propellant burner were taken with K-band microwaves in conjunction with two-color pyrometer and sound-intensity measurements.

THEORY

Unbounded Absorber

Electromagnetic waves passing through an unbounded isotropic medium of free charged particles are attenuated exponentially:

$$P = P_0 e^{-\gamma z} = P_0 e^{-A} \quad (1)$$

(All symbols used in the text are defined in appendix A.)

From classical electromagnetic theory (refs. 4 and 5 and appendix B), it is found that γ , expressed in decibels per centimeter, may be closely approximated by:

$$\gamma \approx \frac{0.455ng}{\omega^2 + g^2} \quad (2)$$

where n is in electrons per cubic centimeter and ω and g are in reciprocal seconds.

Margenau (ref. 6), using an energy-distribution equation instead of the mono-energetic differential equation, obtains substantially the same equation in the region of radiation frequency and electron density of interest as was obtained in this paper.

In equation (2), g is a viscous damping factor due to the collisions between electrons and molecules. With the use of equation (2), the value of g can be determined experimentally by simultaneous measurements of the attenuation at two wavelengths

$$g \approx \sqrt{\frac{\omega_2^2 r_2 - \omega_1^2 r_1}{r_1 - r_2}} \quad (3)$$

This method was used to determine g in this report. Classical theory sets g equal to the electron-molecule collision frequency (refs. 1, 2, and 4) which is found from the kinetic theory of gases (ref. 7) as:

$$g \approx pd^2 \sqrt{\frac{\pi}{2mkT}} \quad (4)$$

Additional damping due to ion-electron collisions was calculated from the formula of Smerd and Westfold (ref. 8) and was found to be negligible.

The electron density n of equation (2) can be determined from Saha's equation (refs. 7 and 9, and appendix C) assuming a single alkali salt in an electrically neutral flame:

$$\log \frac{n^2}{N-n} = \log f = 15.385 + \frac{3}{2} \log T - \frac{5040 q_i}{T} \quad (5)$$

where n and N are in reciprocal cubic centimeters, q_i is in electron volts, and T is in degrees Kelvin. A graph of n/N against $\log f/N$ is given in figure 1. In the region $\log f/N < -2$, $n/N \approx \sqrt{f/N}$.

From equations (2) and (5) the variation of the attenuation coefficient γ with temperature T may be obtained. This is demonstrated in figure 2 where the variation of γ with T is shown for different concentrations of sodium salt and for the K-band microwaves.

It is seen from figure 1 that almost all atoms are ionized when $\log f/N > 1$. Above this value the change in attenuation with temperature becomes negligible. The temperature at which $f/N = 10$ may be described as the upper limit of usefulness of this method for measuring the temperature of unbounded flames. In addition, there is an instrument limitation in detecting microwave power which sets practical limits on the applicable electron density at $3 \times 10^{11}/R < n < 3 \times 10^{13}/R$, when R is in centimeters n is in reciprocal cubic centimeters.

In the case of disequilibrium, Saha's equation may still be used if a changed ionization potential is assumed. Belcher and Sugden (refs. 1 and 2) have demonstrated the disequilibrium effects and have proposed side reactions which will modify Saha's equation in a complex way. Assuming for simplicity that the only change taking place is in the ionization potential, then in the region $f/N \ll 1$ the relation between two ionization potentials and the corresponding attenuation coefficients (from eqs. (2) and (5)) is:

$$\log r_1/r_2 = \frac{2520(q_{i,2} - q_{i,1})}{T} \quad (6)$$

The deviation of the experimentally obtained ionization potential from the spectral-line limit value is a measure of the effect of disequilibrium on the ionization process.

Finite Absorber

In equation (2) the absorber is considered unbounded. Since the flame is of finite size, however, two effects will take place: (1) internal reflections due to the discontinuity at the flame boundary (ref. 4), and (2) the effect due to the electron distribution in and the finite circular geometry of the attenuator. The first of these effects was checked theoretically by use of the equations in reference 4 and experimentally by measurements of the reflected beam intensities; the effect was found to be negligible. However, the effects of electron distribution, a finite cylindrical absorber, and a finite beam cannot be neglected.

Assuming a cylindrically symmetric attenuator traversed normally by a beam of square symmetry, the corrected attenuation coefficient A_c , as a function of the parameters γ and \bar{x}/R , is defined by:

$$A_c = 2R\gamma_c = -10 \log \frac{\text{total transmitted power}}{\text{total incident power}} \quad (7)$$

where A_c is in decibels, \bar{x} is one-half the mean width of the microwave beam, and R is the specific measured radius as shown in figure 3.

The corrected attenuation was calculated assuming the electron density to be a function of the flame radial distance. Shown in figure 3(a) is the electron density distribution for the specific case of the blast burner determined from electrical probe and corrected thermocouple probe measurements. Figure 3(b) shows a more general case assumed for a turbulent flame in thermal equilibrium. The microwave beam power pattern used is shown in figure 4, as determined by actual measurements for a beam emanating from a double concave lens and horn combination. This pattern was found to have almost the same shape in both the E and the H planes. The center line of the microwave beam was assumed to pass through the center of the cylinder and the direction of propagation was taken as normal to the axis of cylindrical symmetry. Because of the complexity of the problem, the integration was done numerically. The flame width, beam width, and flame conductivity are fixed by the flame geometry and by the given values of the parameters A and \bar{x}/R . The quantity A is determined by assuming a homogeneous distribution of salt and a uniform temperature. The curves in figure 5 correct the attenuation for both the salt distribution and the flame geometry. The resulting relation among A_c , A , and \bar{x}/R is shown in figure 5.

For the finite absorber, the value of f/N for the upper limit of usefulness for temperature measurement is more complex than the limit for an infinite absorber. A fair approximation taken from plotting corrected attenuation curves may be given as $f/N \approx 10^{A_c/A}$.

Temperature Measurement Sensitivity

With the insertion of values in the equations shown in appendix D, it was found that in the region used the sensitivity of the instrument to temperature was 4 to 15 times larger than the sensitivity to any other flame parameter such as flame radius, salt flow, flame velocity, or beam size. Since the coefficients B and C (appendix D) as shown in figure 6 are larger for greater values of \bar{x}/R , the final effect is to lower the temperature sensitivity as \bar{x}/R increases until, in the region $\bar{x}/R = 1.8$, the instrument is no longer a good temperature-sensing device.

Because of the similarity in slope and spacing of the correction curves in figure 5, the parameters B and C derived from figure 5(b) may also be employed to estimate the sensitivity of the temperature measurements on the blast burner flame.

If a temperature change ΔT rather than the absolute temperature T is to be measured, an approximate expression for the uncertainty in such a measurement is given by:

$$\frac{\delta(\Delta T)}{\Delta T} \approx 2 \frac{\delta T}{T} + \frac{\delta(\Delta A_c)}{\Delta A_c} \quad (8)$$

More exact expressions for this uncertainty are given in appendix D.

To simplify the reduction of data, an additional requirement for the measurement of fluctuating temperatures is that the change in intensity with temperature change be as linear as possible over the temperature range. The extent of this linearity is demonstrated in figure 7 where graphs of the attenuation as a function of temperature are plotted for five elements.

The response of the system to time-fluctuating temperatures will depend upon the frequency and the velocity of propagation of these fluctuations. Assuming that the attenuation fluctuation moves at the gas-stream velocity u and varies sinusoidally with time at frequency v , the frequency v_l at which the indication of amplitude of the alternating components of power will be reduced 1 decibel is given by:

$$v_l = 0.18 \frac{u}{x} \quad (9)$$

EXPERIMENTAL METHODS

Procedure for Temperature Measurement

Attenuation readings were taken of the flame with and without a known amount of salt added. If the attenuation without added salt could not be neglected (which happened only with the alcohol-oxygen flame), the attenuation with added salt was corrected by means of equation (C2). The temperature was found graphically from curves of attenuation against temperature obtained from equations (5) and (2) and figures 1 and 5. An example showing the steps used may be found in appendix E.

Instrumentation

A schematic diagram of the measuring system is shown in figure 8. The microwave generator for the X-band measurements was a U.S. Navy TS-120 test set containing a 723-A/B Klystron oscillating at 9650 ± 70 megacycles. The microwave generator for the K-band measurements was a power supply of NACA construction with a 2K 33 Klystron oscillating at $27,600 \pm 100$ megacycles. The reflector voltages of both Klystrons were modulated.

Measurements of the beam intensity patterns showed that in order to make the system applicable to flames of the size used, it would be necessary to narrow the beam by means of double-concave metal converging lenses. The lenses used were of aluminum sheet in Lucite holders, designed from information in reference 10. The values of \bar{x} obtained were 1.8 centimeters for the K-band and 3.2 centimeters for the X-band. The distance between lenses was approximately 40 centimeters, with the flame midway between lenses. Attenuation of the beam by ionized flames did not change the voltage standing wave ratio by any detectable amount.

Silicon diode crystals were used as square-law detectors. A 1N26 crystal was used for the K-band (1.25-cm wavelength) and a 1N23 crystal for the X-band (3-cm wavelength) measurements. Two methods were used at various times for measuring the crystal outputs: a tuned voltmeter reading in decibels (with 1 kilocycle modulation on the Klystron) for measuring mean temperatures; and an amplifier, band-pass filter, and cathode ray oscilloscope system (with 20-kilocycle modulation on the Klystron) for recording varying flame temperatures.

Blast-Burner Tests

A blast burner which burned propane-air-oxygen mixtures was used for the experiments. By varying the fuel-oxidant ratio the temperature could be varied from 1900° to 2500° K. The burner was mounted on a large optical bench in such a way that it could be moved to intercept either the K-band or the X-band beams.

The alkali elements were introduced as water solutions of halide salts in a fine spray at the base of the flame. Readings of attenuation by the flame were made with and without the spray. The atomic flow rate was found by measuring the weight of the solution used over a given period of time, the flow rate being kept constant. The flame volume flow rate was found from integrations of total-pressure measurements taken across a number of flames. The average atomic density was obtained by dividing the atomic flow rate by the flame volume flow rate. As the salt was not uniformly distributed throughout the flame, a method was devised by which the magnitude and the shape of the electron density curve in the region below 2100° K could be estimated. An ionization probe with a separation of 2 centimeters between poles was moved through the flame and both current and voltage were measured; from reference 11, $n \propto i/U_e V$. Because of the unknown values of electron mobility and field strength only the relative electron densities could be determined. At the same time, thermocouple temperature measurements were taken to determine the relative temperature profile of the flame. To correct for radiation effects, the thermocouple readings were raised until the peak reading equaled the sodium-line reversal temperature. From these data a curve of the relative atomic density could be obtained. By integrating and normalizing this curve over the flame cross section, a value was obtained for the ratio of the peak electron density to the average

electron density computed from the salt flow rate for the assumption of uniform temperature and salt distribution.

The width of the flame was measured in three different ways: (1) by means of a platinum probe connected to a commercial electronic switch which closed when the resistance between the probe ends was less than 2 megohms; (2) from total-pressure measurements with a probe; and (3) by means of a salt-coated pyrex tube, the salt being melted from the tube when placed across the flame.

To ascertain the temperature of the flame by the sodium-line reversal method (ref. 12), the sodium was introduced as NaNO_3 powder at the flame base.

The blast burner was used to determine the electron collision frequency by use of equation (3) and the ionization potentials by use of equation (6) and to check the correction technique.

Liquid-Propellant Burner

A photograph of the apparatus in the burner cell is shown in figure 9.

The propellants (alcohol-oxygen, and heptane-oxygen that contained a small amount of turpentine) were ignited in a tube 5.1 centimeters in diameter which was open at one end. The temperature range of 2200° to 2900° K was obtained by varying the oxidant-fuel mass flow ratio in discrete steps of 1.2, 1.6, 2.0, and 2.4. The propellant flow was held constant at 0.2 pound per second. The microwave beam was "focused" in the exhaust, 8 to 18 centimeters below the tube end. Because of space limitations, it was possible to use only one wavelength at a time. Both wavelengths were used in measurements on the alcohol-oxygen system, while only K-band measurements were taken on the heptane-oxygen system.

The liquid-propellant burner was used to establish the feasibility of using the microwave apparatus on such types of flames and to obtain data on the rapid fluctuation of temperatures in flames.

The salt used, NaI , was introduced directly into the fuel. The salt was easily soluble in the alcohol, but not in heptane. Thus, it was necessary first to dissolve the NaI in acetone and then to suspend this solution in the heptane. Other alkali salts were tried with unsatisfactory results as to mixing. Since from prior experiments an unknown amount of sodium salt contaminated the alcohol-oxygen flame, equation (C2) was used in determining the temperature.

3109

Temperature measurements were also made in the upper part of the tube for an oxygen-alcohol flame by sodium-line reversal (ref. 13) and at the level of the microwave beam for the heptane-oxygen flame by the two-color pyrometer system (ref. 14).

EXPERIMENTAL RESULTS

Blast Burner

Determination of correction for electron distribution. - Typical data taken with an ionization probe and with a thermocouple probe are shown in figure 10. From averages of such curves the shape of the electron-density curve (fig. 3(a)) was determined. The absolute magnitude of the curve was determined by equating the area integral of the normalized electron density curve to the average electron density calculated from the measured gas flow, salt flow, and sodium-line reversal temperature. The ratio of the maximum electron density to the electron density, assuming a homogeneous distribution of salt, was found to be 0.55. From this curve, the geometry correction for the specific case of the blast burner flame has been determined as shown in figure 5(a).

A partial experimental verification of equation (8) for absorption by a finite-size flame was found by means of measurements in the X-band region with no lenses, one lens, and two lenses. The ratios of experimentally measured attenuations for these three conditions were 0.64:0.77:1.0, respectively, while calculations by means of figure 5(a) predicted ratios of 0.40:0.80:1.0. The discrepancy in the results when no lenses were used is due to the inability of the correction to compensate fully for such a large ratio of \bar{x}/R .

Determination of collision frequency. - From simultaneous attenuation readings on the blast burner in the region $T = 2200^\circ$ K, the ratio of γ for the X-band microwaves to γ for the K-band microwaves, after correction for beam size, was found to be equal to 1.65. Insertion of this value in equation (3) along with known values of the microwave frequencies gave a value of $g = 1.9 \times 10^{11}$ sec⁻¹. This value may be compared with the kinetic theory value of $g = 0.8 \times 10^{11}$ sec⁻¹ (eq. 3), the one determined from the electron mobility (eq. (B14)) as used by Wilson (refs. 11 and 15) in flame ionization studies of $g = 5.9 \times 10^{11}$ sec⁻¹, and the one determined experimentally from microwave attenuations by Belcher and Sugden (refs. 1 and 2) of $g = 0.9 \times 10^{11}$ sec⁻¹. In the region $0.8 \times 10^{11} < g < 2 \times 10^{11}$, K-band attenuation readings are fairly insensitive to the collision frequency g , while the X-band attenuation in this same region is approximately proportional to $1/g$.

In extending the value of collision frequency to other temperature regions beyond that in which measurements were made, it was assumed that $g \propto p/\sqrt{T}$ as in equation (4).

Determination of effective ionization potential. - The total-pressure profiles of 27 different flames were measured. From these profiles and the temperature profile (fig. 10), the integrated volume flow rate was obtained as a function of the sodium-line reversal temperature (fig. 11(a)). The value of $2R$ was found from flame-width measurement by three methods and is shown in figure 11(b) as 5.7 centimeters.

The theoretical attenuation coefficient at 2000° K for the accepted ionization potentials (ref. 16) was calculated. From average values of the K-band attenuation at 2000° K, the effective ionization potentials were found from equation (6) and are shown for four elements (cesium, rubidium, potassium, and sodium) in table I. Also shown are the values found by Wilson (ref. 16) and Belcher and Sugden (ref. 2) using the g employed in their writings and using the g of this report. The effect of changing the g is to raise Wilson's results by about 0.4 ev and to lower Belcher and Sugden's value by about 0.2 ev.

It can be seen from table I that sodium seems unaffected by flame chemistry or disequilibrium and that the stronger the binding of the electron the smaller are the effects.

From the experimentally obtained ionization potentials for cesium, rubidium, and potassium and the accepted value for sodium, the microwave temperatures were obtained by the procedure outlined in appendix E. The resultant temperatures are plotted against the sodium-line temperatures in figure 12.

From figures 11(a) and 11(b) the probable errors in atom density and flame width are $\Delta N/N \approx \pm 0.10$ and $\Delta R/R \approx \pm 0.15$. The uncertainty in the sodium-line reversal temperature was taken as $\Delta T/T \approx \pm 0.01$. When these values and the values of the parameters q_1 , B , and C are inserted into equation (D6), the average deviation expected between sodium-line reversal temperatures and microwave temperatures should range from about $\pm 35^{\circ}$ K at 1900° K to about $\pm 70^{\circ}$ K at 2400° K. Of the K-band and X-band points, 81 and 67 percent, respectively, in figure 12 fall within these limits. However, there is a small systematic error in the X-band tests. It is suggested that this error is probably due either to failure of the theory to correct the attenuation completely for flame geometry in the higher attenuation regions or to the strong dependence of the X-band attenuation on the electron collision frequency. Thus some of the advantage that an X-band system enjoys due to larger and more available components is offset by the larger beam size and the collision frequency dependence.

As is seen from figure 12, there is no apparent dependence of the ionization potential upon the oxygen-nitrogen ratio in the flame. It can be concluded that sodium can be used in a hydrocarbon flame with the accepted value of the ionization potential in Saha's equation.

Liquid Propellant Burner

Mean temperature measurements. - In the case of the liquid propellant burner, fewer individual measurements were made than for the other burners. The flame width measured from photographs was 7.6 centimeters. The flame velocity calculated from high-speed photographs of a screaming condition and from the frequency response (eq. (9)) was 3×10^4 centimeters per second, giving a flow rate of 1.36×10^6 cubic centimeters per second. If an average molecular weight of the exhaust gas of 15 is assumed, a flow rate of 1.2×10^6 cubic centimeters per second is found from the propellant flow rate. A value of 1.3×10^6 cubic centimeters per second was used in the computations. The amount of salt placed in the fuel varied from 0.4 to 1.0 grams in 4000 cubic centimeters of fuel. Atomic densities in the exhaust varied from 1.0 to 1.7×10^{13} atoms per cubic centimeter. The temperature measurements on the oxygen-alcohol burner shown in table II were found by averaging the results of microwave voltmeter readings of numerous runs for given fuel-oxygen mass-flow ratios. The average difference between the two results is 60° K. Use of the classical collision frequency of $g \approx 0.8 \times 10^{11}$ raises the difference between the two results to about 200° K, well outside the experimental error. On the oxygen-heptane burner, averages over short, randomly-spaced intervals were taken by use of the cathode-ray oscilloscope apparatus. The results for K-band microwaves are compared with average "two-color" measurements in figure 13.

Measurement of temperature fluctuations. - When the crystal output was connected to the plates of a cathode-ray oscilloscope, the rapid fluctuations in the attenuation could be observed. Use of equation (9) shows that X-band microwaves would be unsatisfactory in measuring fluctuating temperatures in this flame; therefore only K-band data were taken. A test was made to decide whether the fluctuations were primarily due to temperature changes or to salt density changes. The test was based on the fact that, with a low concentration of cesium salt in the flame at the temperature of the liquid-propellant burner flame, the salt would be almost totally ionized and any large variation in the attenuation would be attributable to flow variations. This experiment was performed and yielded only small attenuation variations at those fuel mixture settings at which injection of sodium salt yielded violent attenuation fluctuations. These results indicated that the observed attenuation fluctuations were due almost entirely to temperature fluctuations and not to changes in the gas flow rate.

Figure 14 shows measurements on the heptane-oxygen burner of temperatures obtained by K-band microwave attenuation measurements, and by the two-color pyrometer. Also shown are simultaneous sound-intensity measurements taken with a microphone 15 centimeters away from the burner. As the response of the microphone for the conditions used is not definitely known, the microphone data are included only to show that screaming conditions existed during the measurement.

3
601CCV-2
Jack

If both the mean temperature and the measured change in attenuation are estimated to be accurate within 2 percent, the error in the change in temperature is 4.5 percent. Figures 14(a) and 14(b) represent conditions of screaming at 1000 and 3000 cycles per second, respectively. The two-color instrument shows higher frequency fluctuations than the microwave instrument because the latter averages over a volume 100 times as great as that covered by the former. Two longer measurement periods are shown in figure 15 for the sound and K-band microwaves. Additional data may be found in reference 14.

In the figures the flow rate and the flame radius were assumed constant for the microwave data, and no correction was made for the frequency response to attenuation fluctuations. Taking the effect of these into account, it is estimated that for 1000 cycles per second screaming the temperature peaks are 20° K low, the valleys 20° K high, and no change occurs in the rest of the curve.

3109

Effects of Addition of Salt Solutions on Flames

The addition of the water-salt solution to the blast flame was observed to change the region of flame stability and to change the flame sound. The effects could nearly be duplicated by using a pure water spray.

When alcohol and oxygen were used in the liquid-propellant burner, the addition of salt had no noticeable effect on the flame except to color it yellow. In the case of heptane-oxygen, the addition of acetone in which sodium iodide was dissolved was found to have a decided effect. With no acetone, steady screaming was observed only at an oxygen-fuel mass-flow ratio $O/F = 1.6$; with 3 percent acetone in the fuel, screaming was observed at $O/F = 1.6$ and 2.0. With 8 percent acetone, the burner screamed at $O/F = 1.2$, 1.6, 2.0, and 2.4. The amount of acetone used in the temperature-determination experiments was always 3 percent or less.

CONCLUSIONS

The following conclusions may be drawn from the experimental and theoretical investigation of flame temperatures by microwave absorption:

1. Theoretical computations indicate that microwave attenuations can be used as a measure of both mean and rapidly fluctuating temperatures, with little dependence upon gas flow. Experimental studies verify these computations within the error of the measurements. Over the range used, the theoretical sensitivity of the attenuation to temperature was estimated to be 5 to 15 times larger than the sensitivity to any other flame parameter.

2. The experimentally obtained collision frequency for electrons was found to be approximately 1.9×10^{11} reciprocal seconds at a temperature of 2200° K.

3. The ionization of sodium seems unaffected by flame chemistry, and the accepted value of the ionization potential may be used. The elements cesium, rubidium, and potassium may be affected by flame chemistry in such a way as to necessitate a calibration by adjusting the values of the ionization potentials. The ionization potentials seem to be independent of the nitrogen-oxygen ratio of the flame.

4. The attenuation formula for an unbounded sheet has been extended to include finite flames. Suitable corrections can be made for the size of the flame if the flame diameter is 60 percent or more of the beam width. Smaller flames introduce serious errors.

5. Microwave temperatures can be read from oscilloscope records by use of a reference scale. Over a temperature span of 600° K (the mid-point depending on the salt used) the variation of intensity with temperature is almost linear. Over this linear range the temperature will be accurate to within about $\pm 60^{\circ}$ K and changes in temperature can be measured within $\pm 5^{\circ}$ K or 4.5 percent of the temperature difference, whichever is larger. The range of the instrument may be increased by the use of a meter with linear decibel scale.

6. The use of K-band radiation was advantageous because of the smaller beam size and the insensitivity of the attenuation to electron collision frequencies.

7. The effect of the addition of the required quantity of salt to the flame has no effect on the combustion properties. However, if additional material is added as a solvent for the salt, the burning may be affected drastically.

Lewis Flight Propulsion Laboratory
National Advisory Committee for Aeronautics
Cleveland, Ohio, May 26, 1954

APPENDIX A

SYMBOLS

The following symbols are used in this report:

A attenuation, $A = 2R\gamma = z\gamma$
A_c corrected attenuation, $A_c = 2R\gamma_c$
B,C parameters
c velocity of light in vacuum, 2.998×10^8 m/sec
d molecular diameter
E electric field strength along the y axis
e electronic charge, 1.602×10^{-19} coulomb
f function in Saha's equation
g viscous damping coefficient (collision frequency)
H magnetic field strength
I intensity of the microwave beam
i ionization probe current
J current density
j $\sqrt{-1}$
k Boltzmann's constant, 8.628×10^{-5} ev/°K or 1.380×10^{-16} erg/°K
m electron mass, 9.107×10^{-31} kg
N number of atoms (per unit volume) furnishing free electrons
n number of free electrons per unit volume
n_i number of positive ions per unit volume
P microwave power
p gas static pressure

300

q_i	ionization potential
R	specific measured flame radius (fig. 2)
r	radial distance vector
T	absolute temperature
t	time
U_e	electron mobility
u	flame velocity
V	ionization probe potential
w	salt mass flow rate
x, y, z	distance vectors
\bar{x}	one-half mean width of the microwave beam
α	phase constant
β	attenuation constant
γ	power attenuation coefficient for an infinite flame
γ_c	power attenuation coefficient for finite flame, db/cm
ϵ	electrical permittivity
ϵ_0	permittivity of free space, 8.85×10^{-12} farad/meter
κ	propagation constant, $\kappa = \alpha + i\beta$
μ	magnetic permeability
μ_0	permeability of free space, 1.257×10^6 henry/meter
ν	cyclic frequency of fluctuation
ν_l	cyclic frequency at which the measurement is down 1 db
σ	electrical conductivity
ω	angular frequency of radiation

Subscripts:

0 initial conditions

1,2,3 used to denote separate conditions appearing in the same
equation

3109

APPENDIX B

DEVELOPMENT OF ATTENUATION EQUATIONS

The following equations are developed in the same sequence as those in reference 4. All units of electrical measurement are rationalized units.

GUTS

The differential equation for a plane wave propagating in the z-direction in an unbounded medium is:

$$\frac{\partial^2 E}{\partial z^2} - \mu\epsilon \frac{\partial^2 E}{\partial t^2} - \mu\sigma \frac{\partial E}{\partial t} = 0 \quad (B1)$$

The equation for H is identical.

If the electromagnetic wave is harmonic in time propagating in the positive z-direction, then the solution of (B1) is given by:

$$E = E_0 \exp(-j\omega t + j\alpha z - \beta z) \quad (B2)$$

GUTS

where

$$\chi^2 = \mu\epsilon\omega^2 + j\mu\sigma\omega = (\alpha + j\beta)^2 \quad (B3)$$

and α is the phase constant and β is the amplitude attenuation constant.

The equation for the displacement of a free electron in a polarized electric field is:

$$m \frac{d^2 y}{dt^2} + mg \frac{dy}{dt} = e E_0 \exp(-j\omega t) \quad (B4)$$

where y is the displacement of the electron from equilibrium and g is a viscous damping factor. The steady-state solution of (B4) is then:

$$y = \frac{1}{g - j\omega} \frac{e}{m} E_0 \exp(-j\omega t) \quad (B5)$$

If there are n free electrons per unit volume, the maximum current density J is:

$$J = ne \frac{dy}{dt} = \left(\frac{ne^2}{g - j\omega} \right) \frac{E}{m} \quad (B6)$$

since $J = \sigma E$, it follows that

$$\sigma = \frac{n \frac{e^2}{m}}{g - j\omega} \quad (B7)$$

Assuming both $\epsilon = \epsilon_0$ and $\mu = \mu_0$, insertion of the value of σ from (B7) into equation (B3) yields β as:

$$\beta = \frac{\omega}{c} \left\{ \frac{1}{2} (1 - \Phi) \left[-1 + \sqrt{1 + \frac{\Phi^2 g^2}{\omega^2 (1 - \Phi)^2}} \right] \right\}^{1/2} \quad (B8)$$

where

$$\Phi = \frac{ne^2}{m\epsilon_0} \left(\frac{1}{\omega^2 + g^2} \right) \quad (B9)$$

For $\Phi \ll 1$, by means of the binomial expansion,

$$\beta \approx \frac{g\Phi}{2c} \left(1 + \frac{\Phi}{2} \right) \quad (B10)$$

In the wavelength and concentration range of interest, β can be further approximated by

$$\beta \approx \frac{g\Phi}{2c} = \frac{e^2}{2cm\epsilon_0} \frac{ng}{\omega^2 + g^2} \quad (B11)$$

Since

$$E \propto e^{-\beta z}$$

or

$$P = P_0 e^{-2\beta z} = P_0 e^{-\gamma z}$$

insertion of numerical values for e , c , m , and ϵ_0 in the proper units yields

$$\gamma \approx \frac{0.455ng}{\omega^2 + g^2} \quad (B12)$$

where γ is in decibels per centimeter, n is in electrons per cubic centimeter, and g is in reciprocal seconds. Equation (B12) may be used up to the region $\gamma \approx 5$ for K-band microwaves and $\gamma \approx 10$ decibels per centimeter for X-band microwaves.

The d-c mobility is defined in reference 7 as

$$U_e = \frac{dy}{dt} \cdot \frac{1}{E} \quad (B13)$$

6012

Substituting from equation (B6) and setting $g \gg \omega$

$$U_e \approx \frac{e}{gm} \quad (B14)$$

CV-3 back

APPENDIX C

SAHA'S EQUATION

Saha's equation (refs. 7 and 9) for alkali elements is given by:

$$f = \frac{nn_i}{N - n_i} = \left(\frac{2\pi mk}{h^2} \right)^{3/2} T^{3/2} \exp \left(\frac{-q_i}{kT} \right) \quad (C1)$$

For a single salt in an electrically neutral flame $n_i = n$ and equation (C1) may be expressed as equation (5).

Of interest is the problem of attenuation measurements of a flame which is contaminated by an unknown quantity of salt. In this case, two attenuations may be measured, γ_1 and γ_2 , the respective attenuations before and after the addition of a known amount of salt. The following equations may be set up:

for contaminating salt in the flame

$$\frac{n_{11}}{N_1 - n_{11}} = f_1$$

for contaminating salt plus known salt

$$\frac{(n_{12} + n_{22}) n_{12}}{N_1 - n_{12}} = f_1$$

$$\frac{(n_{12} + n_{22})(n_{12} + n_{22} - n_{12})}{N_2 - n_{22}} = f_2$$

for known salt only in the flame

$$\frac{n_{23}^2}{N_2 - n_{23}} = f_2$$

where the first subscript refers to the salt and the second to the attenuation reading.

$$n_{12} + n_{22} \propto \gamma_2$$

$$n_{11} \propto \gamma_1$$

Defining

$$r_3 = \frac{0.455n_{23}g}{g^2 + \omega^2}$$

and defining

$$\lim_{f_2 \rightarrow \infty} r_3 = r_T$$

if $n_{11} \approx \sqrt{N_1 f_1}$ and $n_{23} \approx \sqrt{N_2 f_2}$, then

$$r_1^2 + r_3^2 - r_2^2 = 0 \quad (C2)$$

if $f_1 = f_2$, then

$$r_1^2 + r_3^2 - r_2^2 = - (r_1 + r_3 - r_2) f_2 \frac{0.455g}{\omega^2 + g^2} \quad (C3)$$

if $n_{11} \approx N_1$ and $n_{23} \approx \sqrt{N_2 f_2}$, then

$$r_1^2 + r_3^2 - r_2^2 = r_3^2 \left(\frac{r_2 - r_1}{r_T} \right) \quad (C4)$$

APPENDIX D

SENSITIVITY OF TEMPERATURE MEASUREMENT

The following approximate formulas serve to indicate the sensitivity of the microwave temperature method to changes in various parameters and to aid in estimating possible errors. Equations (6) and (2) can be combined to give the dependency of γ on T over the region $f/N < 1$.

$$\gamma \propto \left[\sqrt{N} T^{1/4} \exp\left(-\frac{q_1}{kT}\right) \right] / \omega^2 + g^2 \quad (D1)$$

This dependency may be approximately represented by the proportionality

$$\gamma \propto \sqrt{N} \exp\left(-\frac{q_1}{2kT}\right) \quad (D2)$$

also

$$\gamma = \gamma_c \cdot \gamma/\gamma_c \quad (D3)$$

From equations (D1) and (D2),

$$\frac{\delta T}{T} = \frac{kT}{q_1} \left(\frac{2\delta\gamma}{\gamma} - \frac{\delta N}{N} \right) \quad (D4)$$

and

$$\delta \frac{\gamma}{\gamma_c} = \frac{\partial(\gamma/\gamma_c)}{\partial(\bar{x}/R)} \delta \frac{F}{R} + \frac{\partial(\gamma/\gamma_c)}{\partial A} \delta A \quad (D5)$$

where $A = 2R\gamma$. Combining these equations yields the following relation among the variations in the experimental factors which enter into a temperature determination:

$$\frac{\delta T}{T} \approx \frac{kT}{q_1} \left(\frac{2}{1-B} \frac{\delta \gamma_c}{\gamma_c} - \frac{\delta N}{N} + 2 \frac{B-C}{1-B} \frac{\delta R}{R} + \frac{2C}{1-B} \frac{\delta \bar{x}}{\bar{x}} \right) \quad (D6)$$

where the parameters

$$B = \frac{\partial(\gamma/\gamma_c)}{\partial A} \frac{A}{\gamma/\gamma_c}$$

$$C = \frac{\partial(r/r_c)}{\partial(\bar{x}/R)} \cdot \frac{\bar{x}/R}{r/r_c}$$

are obtained from figure 5(b) and are shown in figure 6 as functions of A_c and \bar{x}/R . Since

$$\frac{\delta r_c}{r_c} = \frac{\delta A_c}{A_c} - \frac{\delta R}{R}$$

NOTE

and

$$\frac{\delta N}{N} \approx \frac{\delta w}{w} - \frac{\delta u}{u} - \frac{2\delta R}{R}$$

then in terms of the salt mass-flow rate w and the flame linear velocity u

$$\frac{\delta T}{T} \approx \frac{kT}{q_i} \left(\frac{2}{1-B} \frac{\delta A_c}{A_c} - \frac{2C}{1-B} \frac{\delta R}{R} - \frac{\delta w}{w} + \frac{\delta u}{u} + \frac{2C}{1-B} \frac{\delta \bar{x}}{\bar{x}} \right) \quad (D7)$$

In the range of usefulness of a single salt, q_i/kT will vary from 20 to 30. By inserting in equation (D7) the extreme values of B and C from figure 6, it is found that the range of the ratio of the sensitivity of the attenuation to temperature to the sensitivity of the attenuation to any other flame parameter is:

\bar{x}/R	Ratio of sensitivity
0.6	10 - 30
1.0	5 - 25
1.4	4 - 15
1.8	3 - 12

From these values it can be said that in the range of attenuations where the instrument was used the attenuation was 5 to 15 times more sensitive to temperature change than to any other flame parameter. The sensitivity to flame radius becomes larger with increasing \bar{x}/R . From these values it can be seen that serious errors will enter when \bar{x}/R is greater than 1.4 and that above $\bar{x}/R = 1.8$ the instrument is unsuited for the determination of temperature.

If the temperature change ΔT from a mean temperature \bar{T} is to be measured by the deviation of the attenuation ΔA_c from the mean attenuation \bar{A}_c , then the sensitivity of the change using equation (D6)

and assuming R , \bar{x} , and N constant is given by

$$\frac{\delta(\Delta T)}{\Delta T} = \frac{\delta(\Delta A_c)}{\Delta A_c} + \frac{2\delta\bar{T}}{\bar{T}} - \frac{\delta\bar{A}_c}{\bar{A}_c} \quad (D8)$$

where $\delta\bar{T}/\bar{T}$ is to be substituted from (D6).

The usual method of determining fluctuations in temperature is by use of previously prepared theoretical curves of intensity ratio against temperature for different values of N . If the mean temperature is determined from these curves and the measured microwave attenuation, then by use of equations (D7) and (D8) the probable error in the temperature fluctuations is given by:

$$\left| \frac{\delta(\Delta T)}{\Delta T} \right|^2 \approx \left| \frac{\delta(\Delta A_c)}{\Delta A_c} \right|^2 + \left(\frac{2k\bar{T}}{q_1} \right)^2 \left[\left| \left(\frac{2}{1-B} - \frac{q_1}{2k\bar{T}} \right) \frac{\delta\bar{A}_c}{\bar{A}_c} \right|^2 + \left| \frac{2C}{1-B} \frac{\delta R}{R} \right|^2 + \left| \frac{\delta_w}{w} \right|^2 + \left| \frac{\delta_u}{u} \right|^2 + \left| \frac{2C}{1-B} \frac{\delta\bar{x}}{\bar{x}} \right|^2 \right] \quad (D9)$$

where the δ 's denote probable errors.

If, however, an independent method of measuring the mean temperature is used then equations (D6) and (D8) yield

$$\left| \frac{\delta(\Delta T)}{\Delta T} \right|^2 \approx \left| \frac{\delta(\Delta A_c)}{\Delta A_c} \right|^2 + \left| \frac{2\delta\bar{T}}{\bar{T}} \right|^2 + \left(\frac{2k\bar{T}}{q_1} \right)^2 \left[\left| \left(\frac{2}{1-B} - \frac{q_1}{2k\bar{T}} \right) \frac{\delta\bar{A}_c}{\bar{A}_c} \right|^2 + \left| \frac{2(C+1-B)}{1-B} \frac{\delta R}{R} \right|^2 + \left| \frac{2C}{1-B} \frac{\delta\bar{x}}{\bar{x}} \right|^2 \right]$$

Since in most cases the mean attenuation is taken from a large number of readings, the terms containing \bar{A}_c may be neglected.

APPENDIX E

EXAMPLE FOR OBTAINING THE TEMPERATURE FROM THE ATTENUATION

If sodium salt and K-band attenuation are used, the experimental attenuation due to the added salt A_c may be changed to A by means of figure 5 and the known value of $\frac{x}{R}$; A is divided by the flame diameter $2R$ to obtain γ , and T is found from figure 2 for the known value of N .

If another salt and/or another microwave frequency is used, the following example gives the procedure by which γ is found as a function of T as in figure 2.

1. The following conditions are assumed:

Flame volume flow rate, cc/sec	10^6
Salt mass flow rate, gm/sec	2.2×10^{-3}
ω (K-band microwaves)	1.73×10^{11}
g	$1.9 \times 10^{11} \sqrt{2200/T} = 8.9 \times 10^{12} / \sqrt{T}$
Salt used	LiI
q_1 , ev	5.36
Molecular weight	133.9

2. Find: γ at 2800° K

$$3. N = \frac{2.2 \times 10^{-3} \times 6.02 \times 10^{23} \times 1}{10^6 \times 133.9} = 10^{13} \text{ atoms of Li/cc}$$

$$4. \log f = 15.385 + \frac{3}{2} \log 2800 - \frac{5040 \times 5.36}{2800} = 10.90 \text{ (eq. (5))}$$

$$\log f/N = -2.10, n/N = 0.089 \text{ (fig. 1)}$$

$$5. \gamma = \frac{0.455 g N}{\omega^2 + g^2} \cdot \frac{n}{N} \text{ (eq. (2))}$$

$$= 13.0 \times n/N = 1.16, \text{ db/cm}$$

By repeating steps 4 and 5 for different temperatures, a graph similar to figure 2 may be plotted. For known values of $\frac{x}{R}$ and R , a graph of the attenuation A_c against the temperature may be plotted with the use of figure 5.

REFERENCES

1. Belcher, H., and Sugden, T. M.: Studies on the Ionization Produced by Metallic Salts in Flames. Pt. I. The determination of the collision frequency of electrons in coal-gas/air flames. Proc. Roy. Soc. (London), ser. A, vol. 201, May 23, 1950, pp. 480-488.
2. Belcher, H., and Sugden, T. M.: Studies on the Ionization Produced by Metallic Salts in Flames. Pt. II. Reactions governed by ionic equilibria in coal-gas/air flames containing alkali metal salts. Proc. Roy. Soc. (London), ser. A, vol. 202, June 1950, pp. 17-39.
3. Rudlin, Leonard: Preliminary Results of a Determination of Temperatures of Flames by Means of K-Band Microwave Attenuation. NACA RM E51G20, 1951.
4. Stratton, Julius Adams: Electromagnetic Theory. McGraw-Hill Book Co., Inc., 1941, pp. 268-277; 325-327; 511-516.
5. Montgomery, C. G., Dicke, R. H., and Purcell, E. M., eds.: Principles of Microwave Circuits. First ed., McGraw-Hill Book Co., Inc., 1948, pp. 393-396.
6. Margenau, H.: Conduction and Dispersion of Ionized Gases. Phys. Rev., vol. 69, 1946, pp. 508-513.
7. Kennard, Earle H.: Kinetic Theory of Gases. McGraw-Hill Book Co., Inc., 1938, pp. 103-105; 426-428; 464-470.
8. Smerd, S. F., and Westfold, K. C.: The Characteristics of Radio-Frequency Radiation in an Ionized Gas, with Application to the Transfer of Radiation in the Solar Atmosphere. Phil. Mag., ser. 7, vol. 40, no. 307, Aug. 1949, pp. 831-848.
9. Saha, Megh N.: A Theory of Physical Phenomena at High Temperatures, with Application to Astrophysics. Chem. Abs., vol. 15, no. 23, Dec. 10, 1921, p. 3934. (Abs. from Zs. f. Phys., vol. 6, 1921, pp. 40-55.)
10. Kock, W. E.: Metal Lens Antennas. Proc. Inst. Radio Eng., vol. 34, no. 11, Nov. 1946, pp. 828-836.
11. Wilson, H. A.: Modern Physics. Third ed., Blackie & Sons, Ltd., 1948, pp. 317-334.
12. Lewis, Bernard, and von Elbe, Guenther: Flame Temperatures. Temperature - Its Measurement and Control in Science and Industry. Reinhold Pub. Corp., 1941, pp. 707-719.

13. Heidmann, M. F., and Priem, R. J.: A Modified Sodium-Line Reversal Technique for the Measurement of Combustion Temperatures in Rocket Engines. *Jour. Am. Rocket Soc.*, vol. 23, no. 4, July-Aug. 1953, pp. 248-253.

14. Heidmann, M. F., and Priem, R. J.: Application of an Electro-Optical Two-Color Pyrometer to Measurement of Flame Temperature for Liquid Oxygen - Hydrocarbon Propellant Combination. NACA TN 3033, 1953.

15. Wilson, H. A.: Electrical Conductivity of Flames. *Rev. Modern Phys.*, vol. 3, no. 1, Jan. 1931, pp. 156-189.

16. Hodgman, Charles D., ed.: *Handbook of Chemistry and Physics*. Thirtieth ed., Chem. Rubber Pub. Co., 1947, pp. 1949-1951.

6012

CV-4 back

TABLE I. - COMPARISON OF IONIZATION POTENTIALS OF ALKALI METALS

Source	Damping factor, sec ⁻¹	Ionization potential, ev					Estimated error, ev
		Cs	Rb	K	Na	Li	
Accepted, reference 16	---	3.87	4.16	4.32	5.12	5.36	±0.01
Present data	1.9×10 ¹¹	4.30	4.37	4.54	5.15	-----	±0.06
Reference 15	5.9 "	3.97	4.22	4.35	4.77	4.88	-----
Reference 15	1.9 "	4.37	4.62	4.77	5.20	5.32	-----
Reference 2	.9 "	-----	-----	4.6	-----	-----	-----
Reference 2	1.9 "	-----	-----	4.4	-----	-----	-----

3109

TABLE II. - MEAN MICROWAVE TEMPERATURES

OF OXYGEN-ALCOHOL BURNER EXHAUST USING

K-BAND AND X-BAND MICROWAVES

Oxidant-fuel mass-flow ratio	K-Band °K	X-Band °K
1.2	2450±40	2420±40
1.6	2490±40	2410±40
2.0	2400±40	2350±40
2.4	2400±40	2310±40

3109

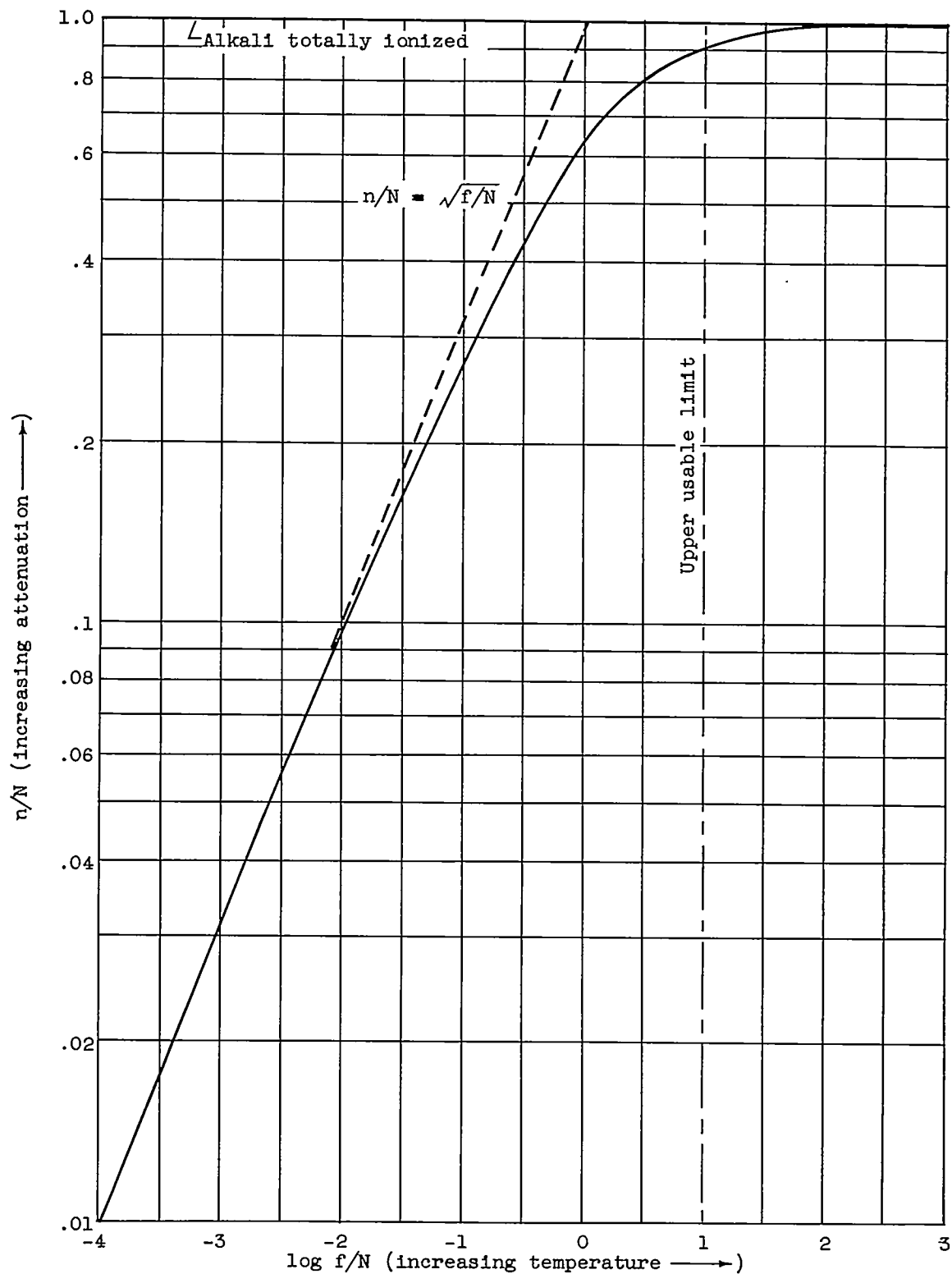


Figure 1. - Ratio n/N as a function of $\log f/N$, by means of Saha's equation (eq. (5)).

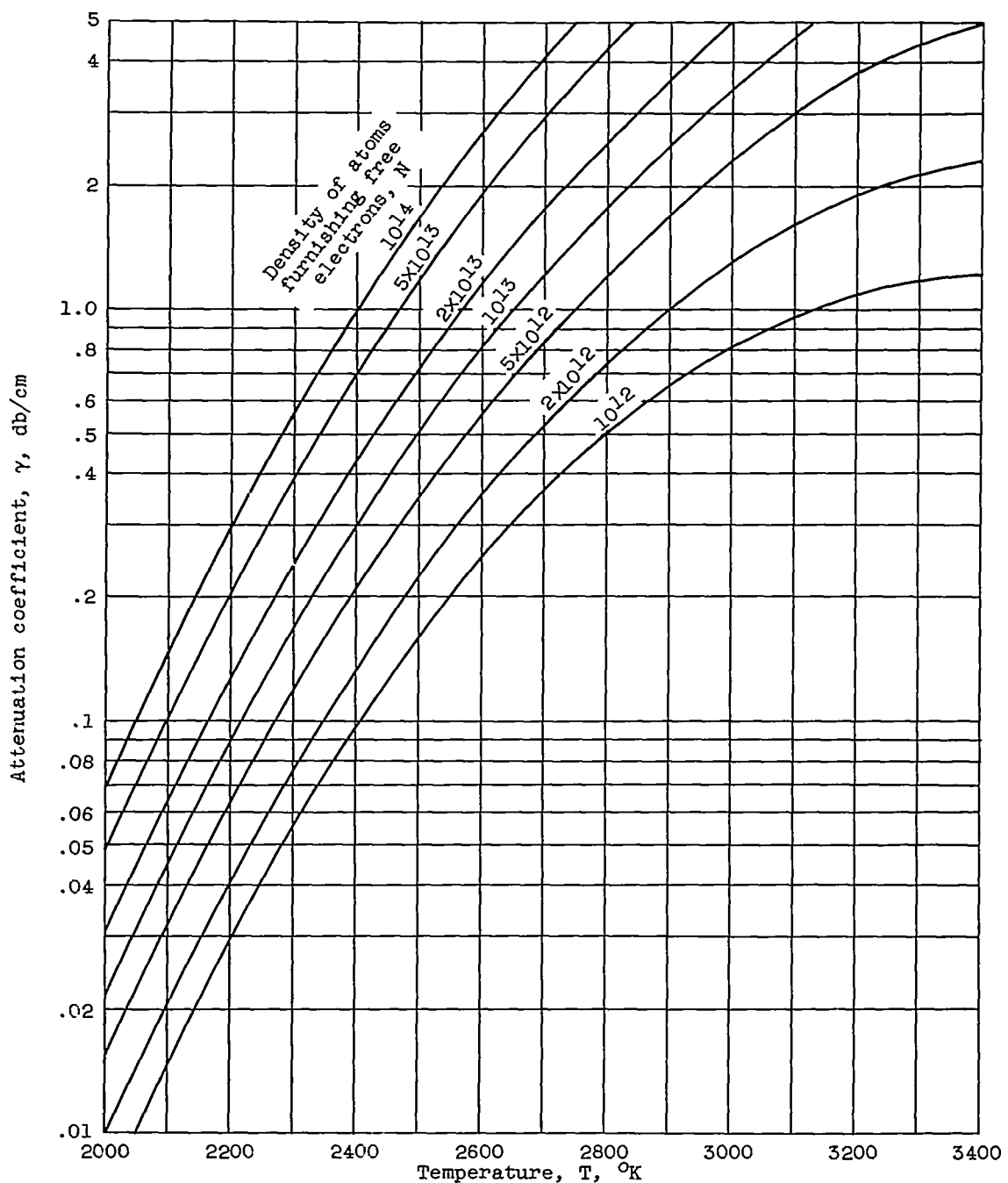
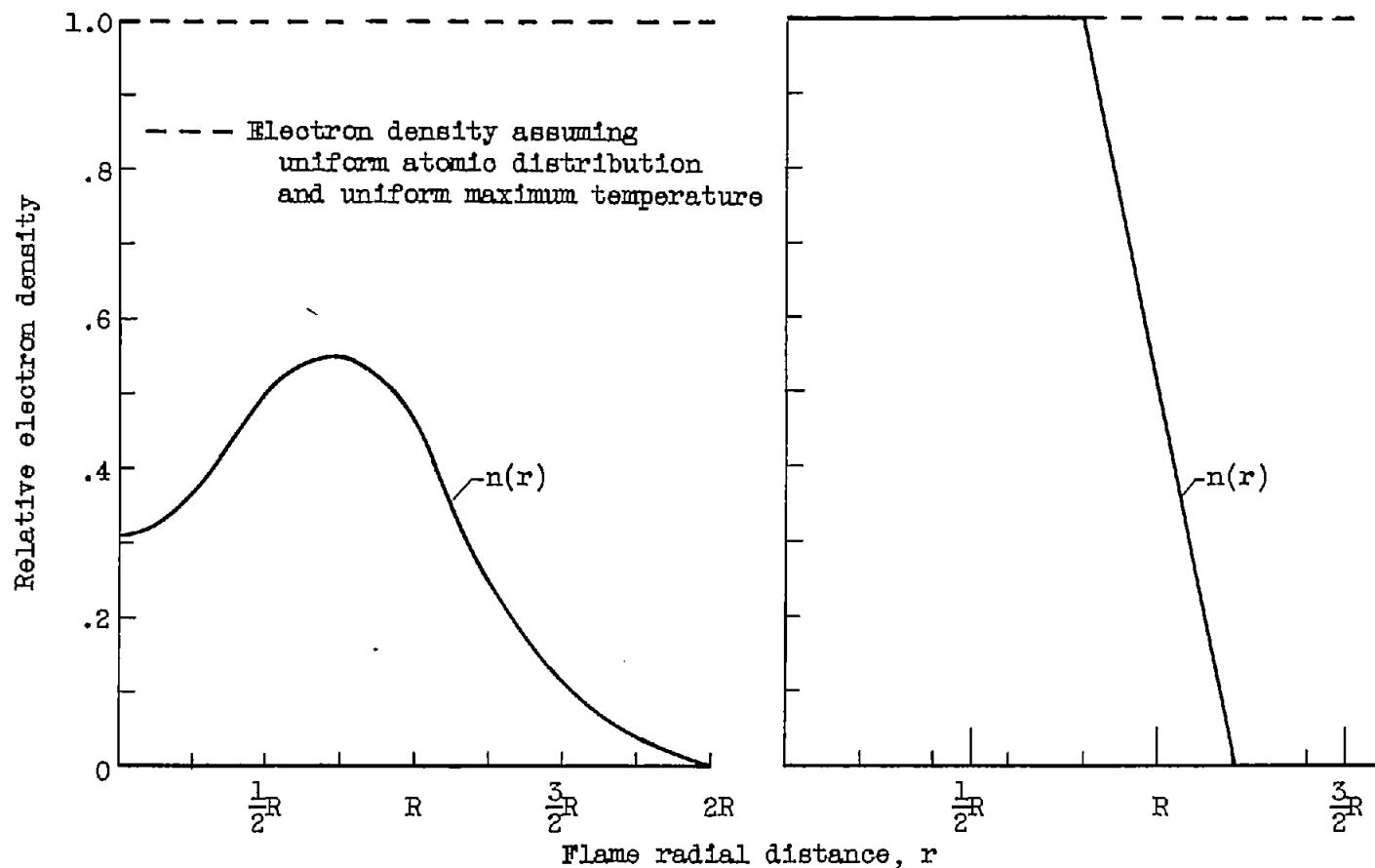


Figure 2. - Attenuation coefficient γ as a function of the temperature for K-band microwaves. Sodium salt; experimental value of g ; different values of N . $\gamma \approx 1.3 \times 10^{-12} N(n/N)$.



(a) Specific case of blast burner taken from measurements of temperature and ionization current in flame.

(b) General case, assumed for liquid propellant burner.

Figure 3. - Electron density as a function of flame radial distance. Used in calculation of flame geometry correction.

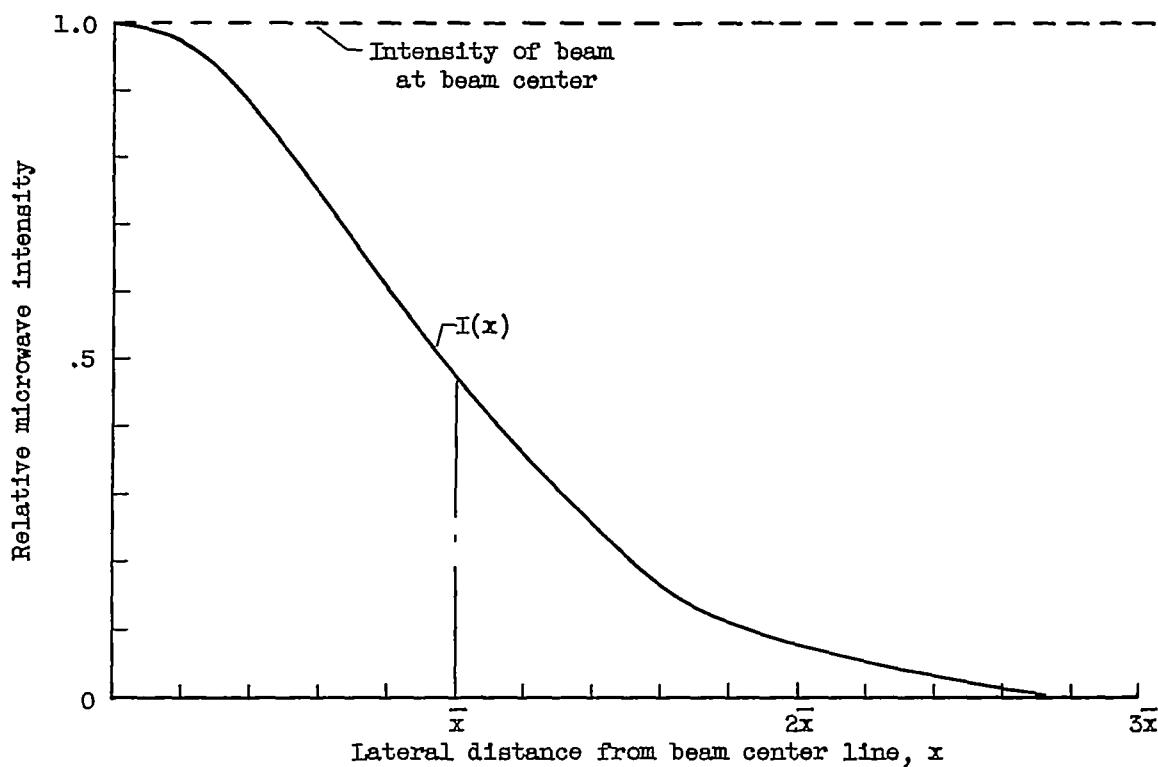
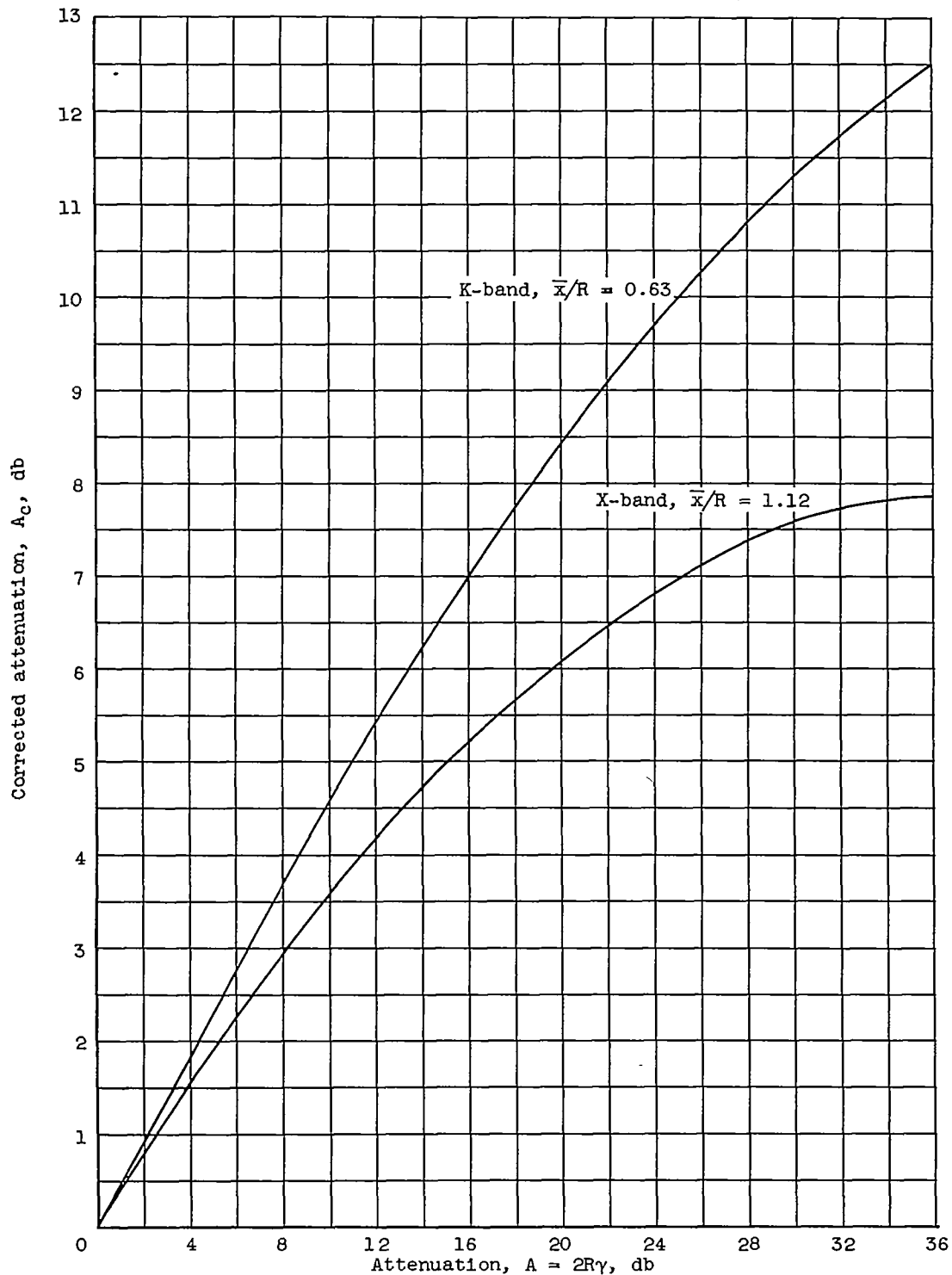


Figure 4. - Measured microwave beam intensity pattern as a function of lateral distance x from beam center line. Used in calculation of flame geometry correction.

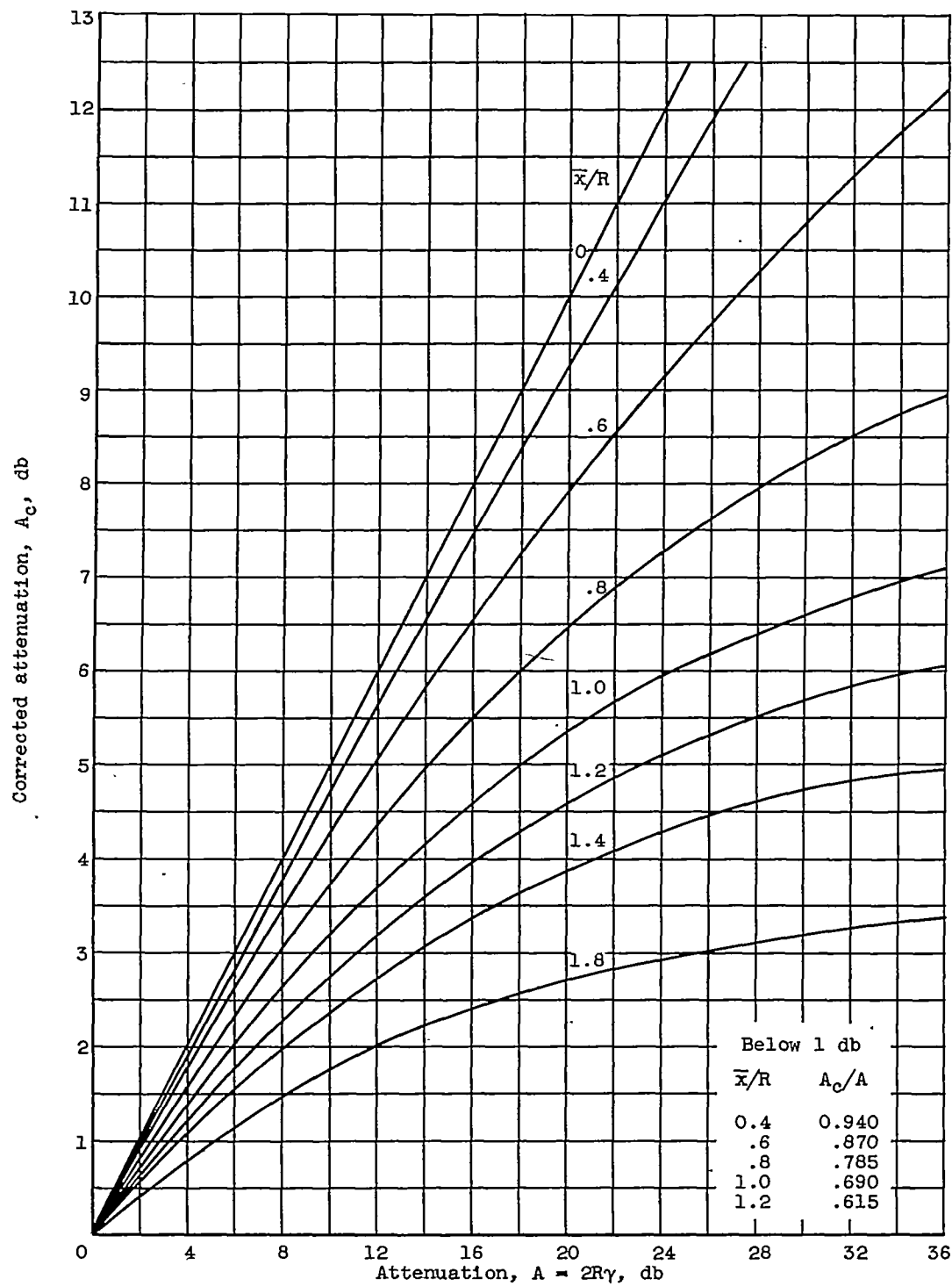
3109

CV-5



(a) Flame geometry for specific case of blast burner (see fig. 3(a)).

Figure 5. - Corrected attenuation A_c as a function of attenuation A for values of the parameter \bar{x}/R .



(b) Flame geometry for general case (see fig. 3(b)).

Figure 5. - Concluded. Corrected attenuation A_c as a function of attenuation A for values of the parameter \bar{x}/R .

3109

CV-5 back

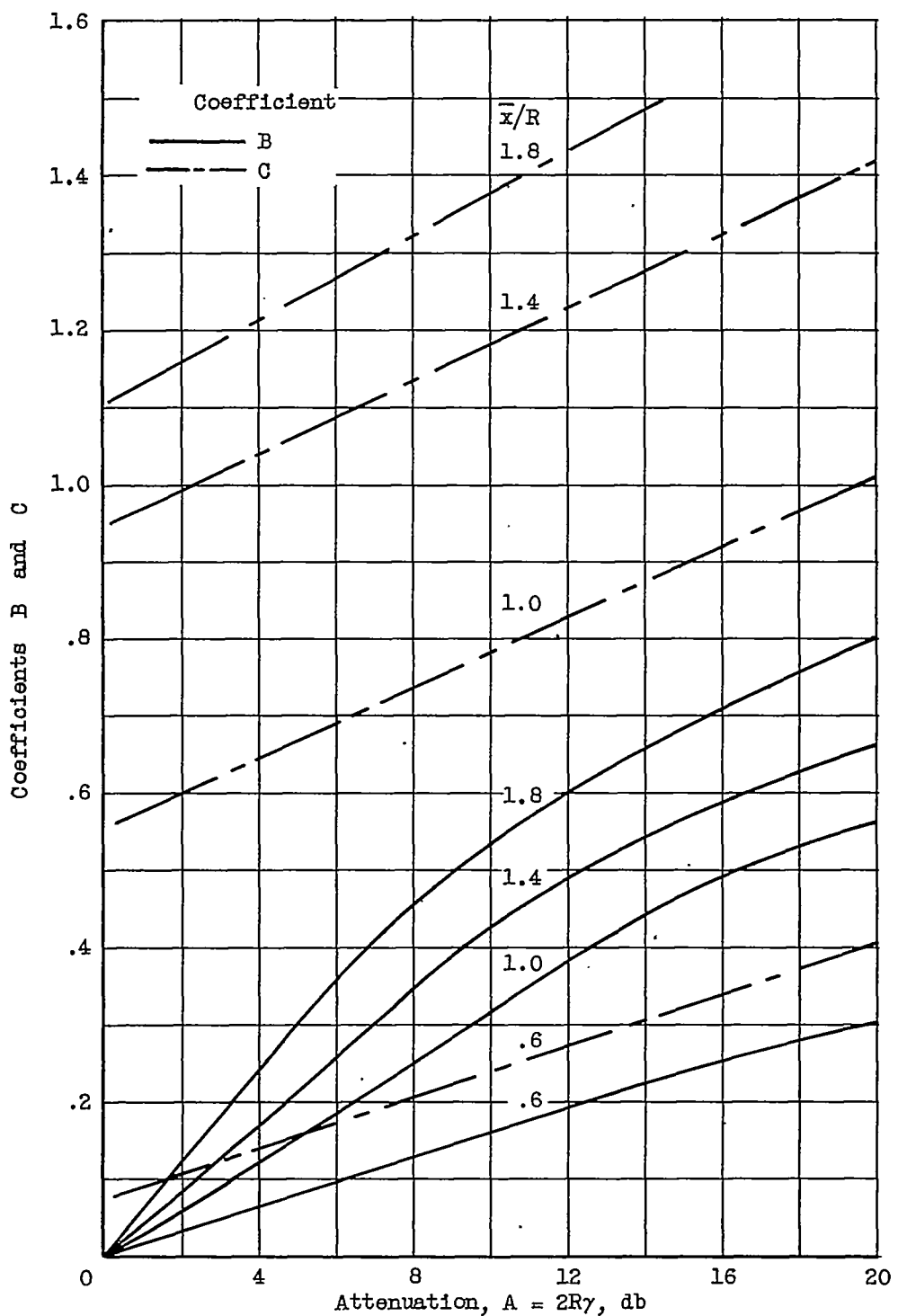


Figure 6. - Coefficients B and C of the sensitivity equations against attenuation A with \bar{x}/R as parameter (fig. 5(b)).

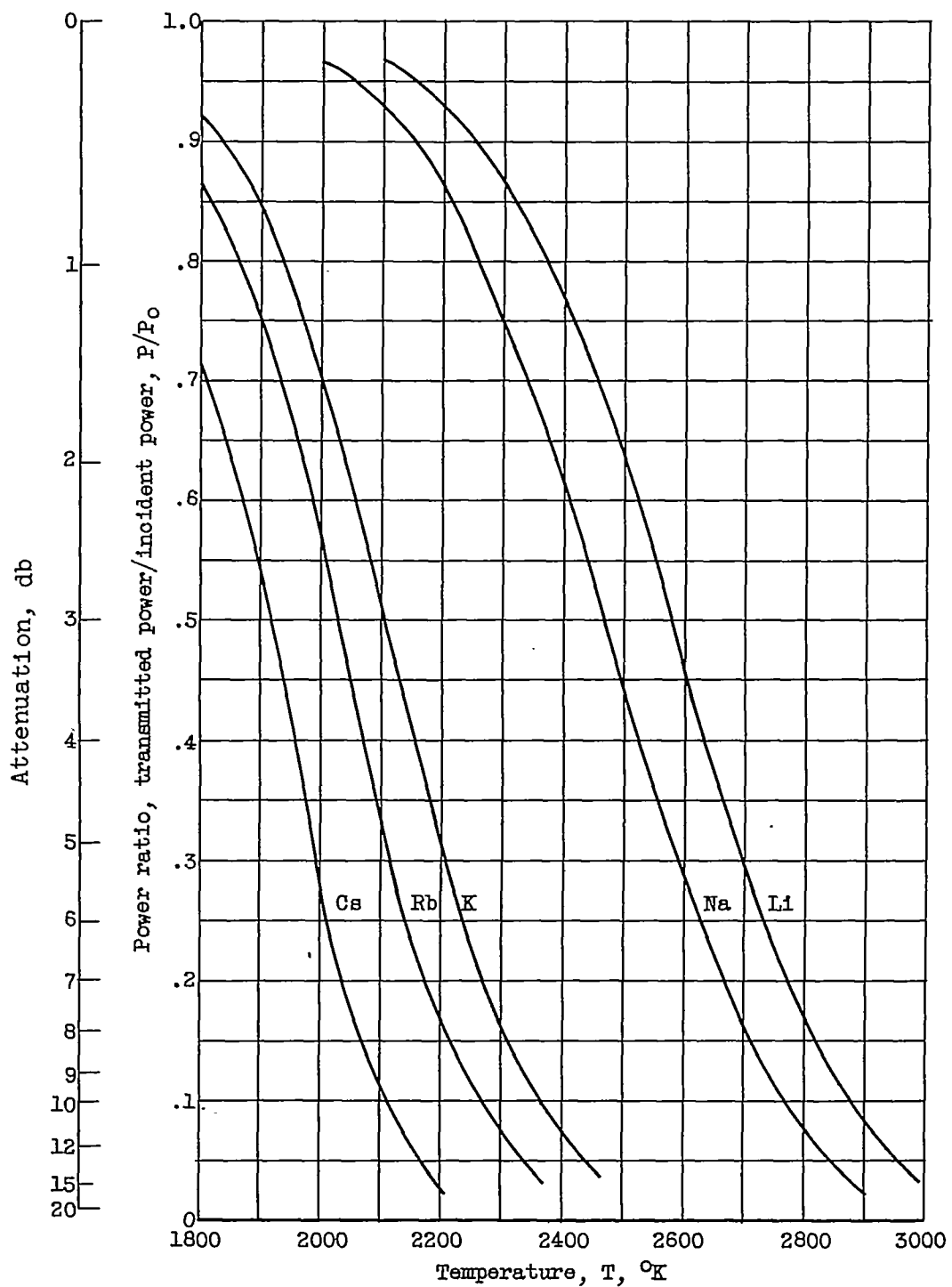


Figure 7. - Theoretical microwave power attenuation for K-band radiation for five elements. $2R = 7.6$ centimeters; $N = 10^{13}$ atoms per cubic centimeter; $g = 1.9 \times 10^{11} \sqrt{\frac{2200}{T}}$; q_i , accepted values.

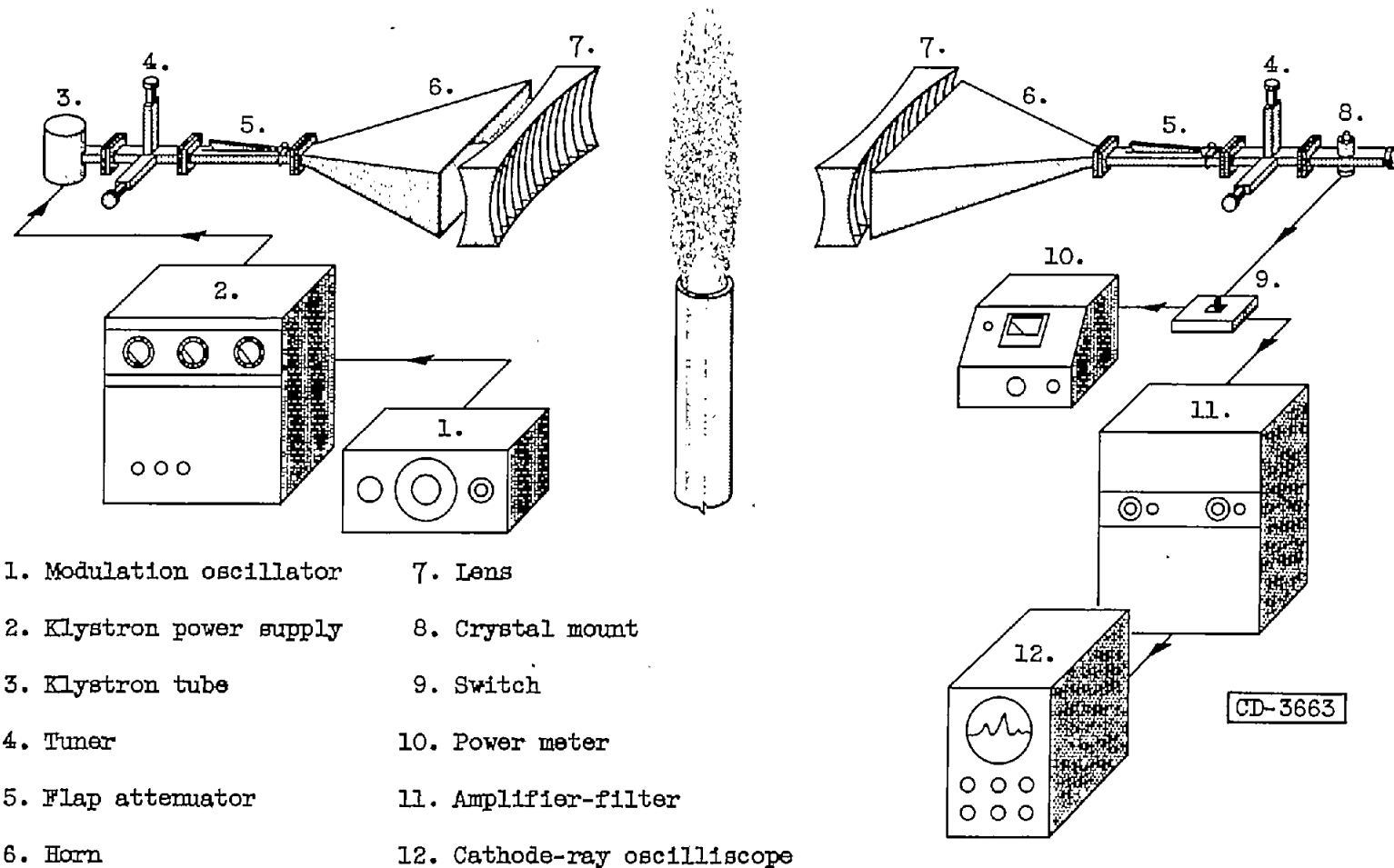


Figure 8. - Schematic diagram of the temperature-measuring apparatus.

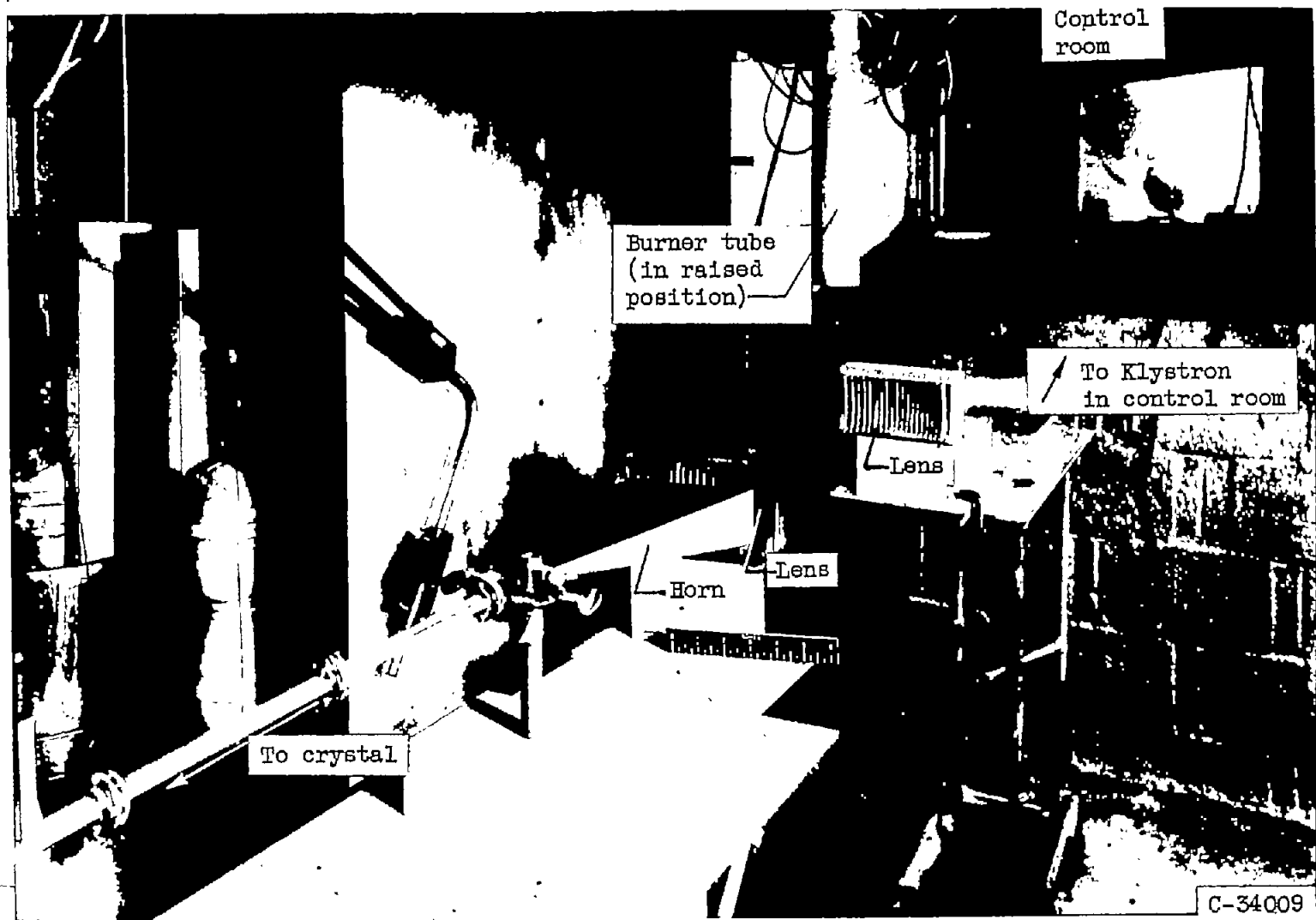


Figure 9. - K-band microwave equipment in the liquid propellant burner test cell.
(electronic equipment in controlroom.)

3109

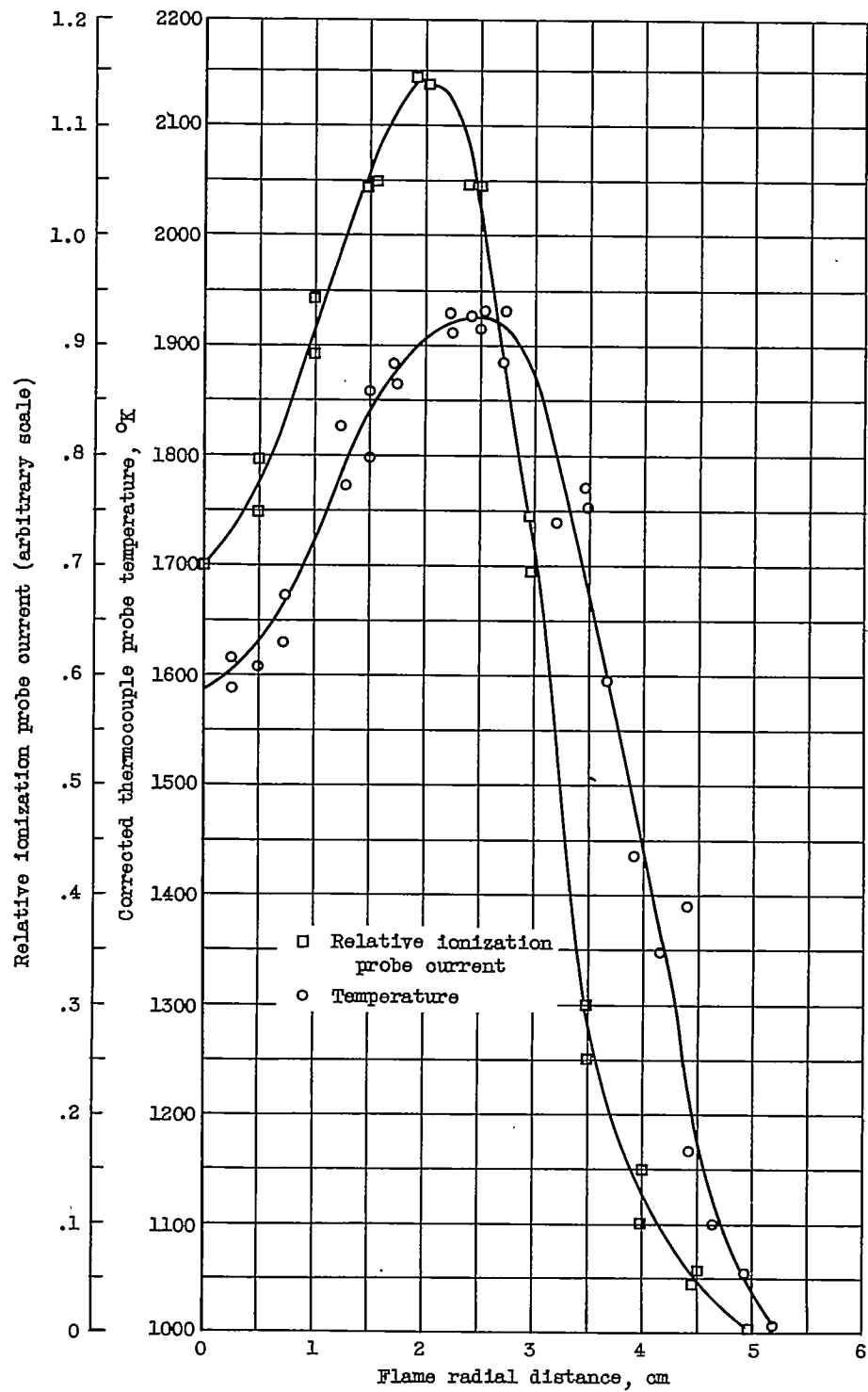


Figure 10. - Typical plots of relative ionization probe current and thermocouple probe temperature across blast burner flame.

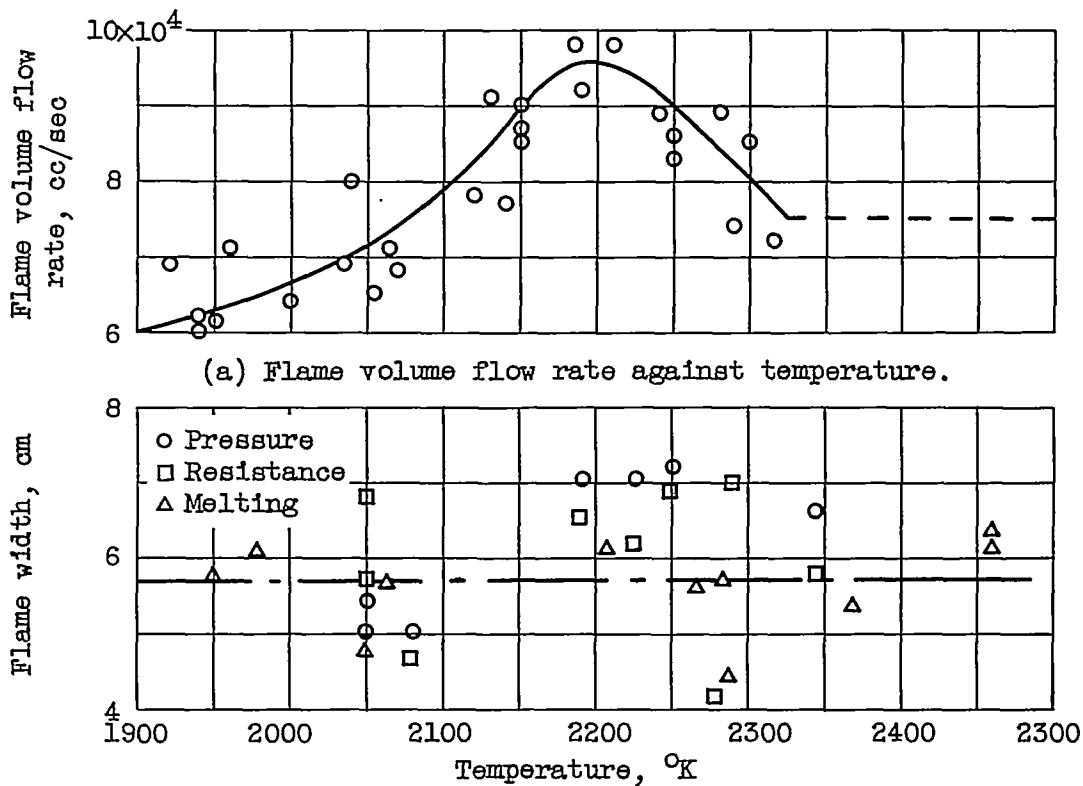
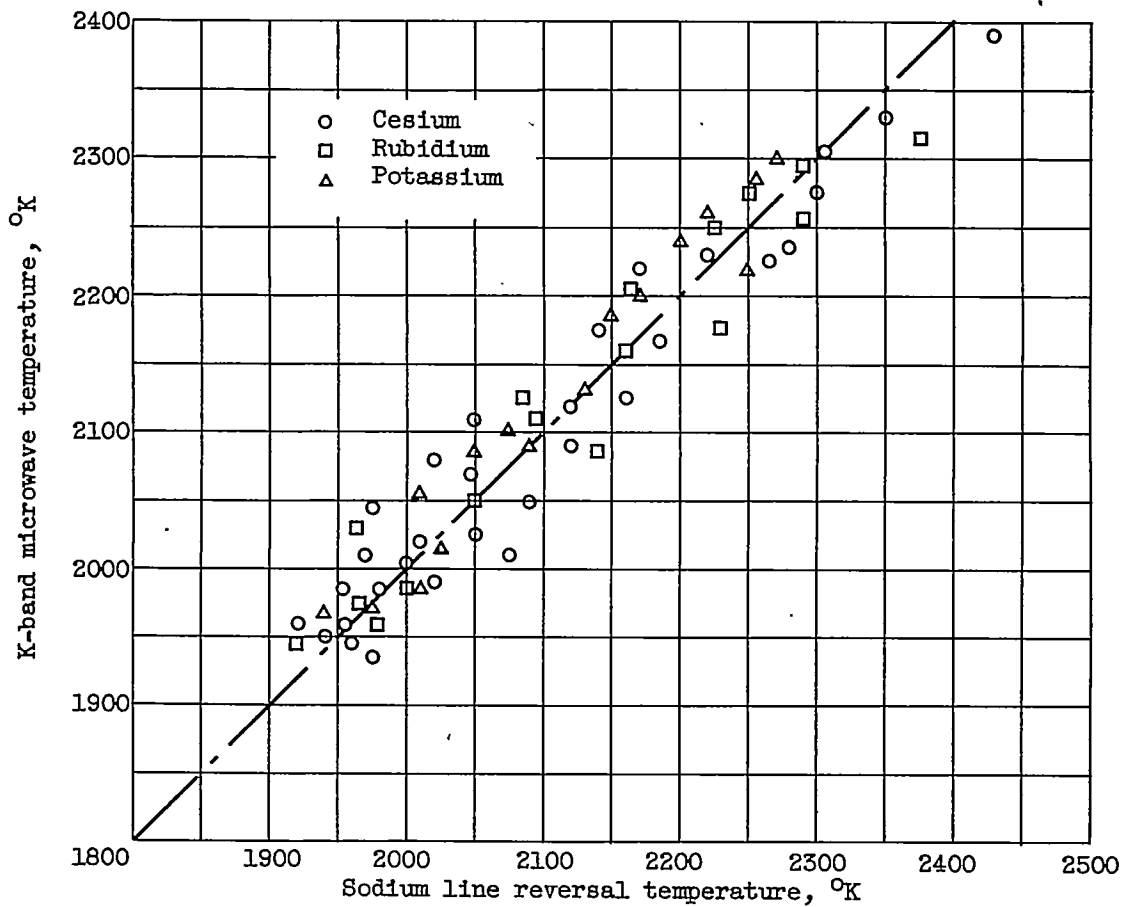


Figure 11. - Experimentally obtained flame parameters of blast burner against sodium line reversal temperatures.

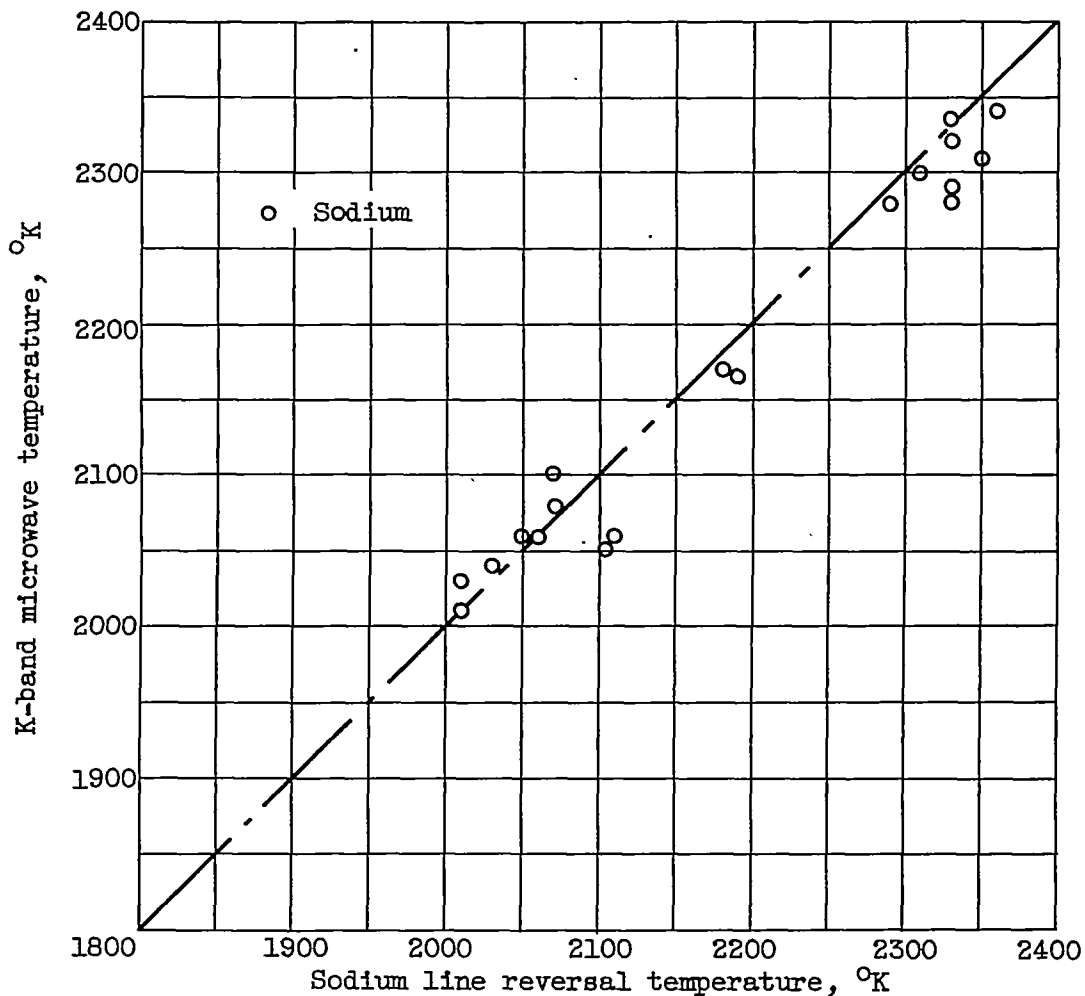
3109

CV-6



(a) K-band microwaves, obtained for experimental ionization potentials for cesium, rubidium, and potassium.

Figure 12. - Microwave temperature against sodium line reversal temperature for blast burner.

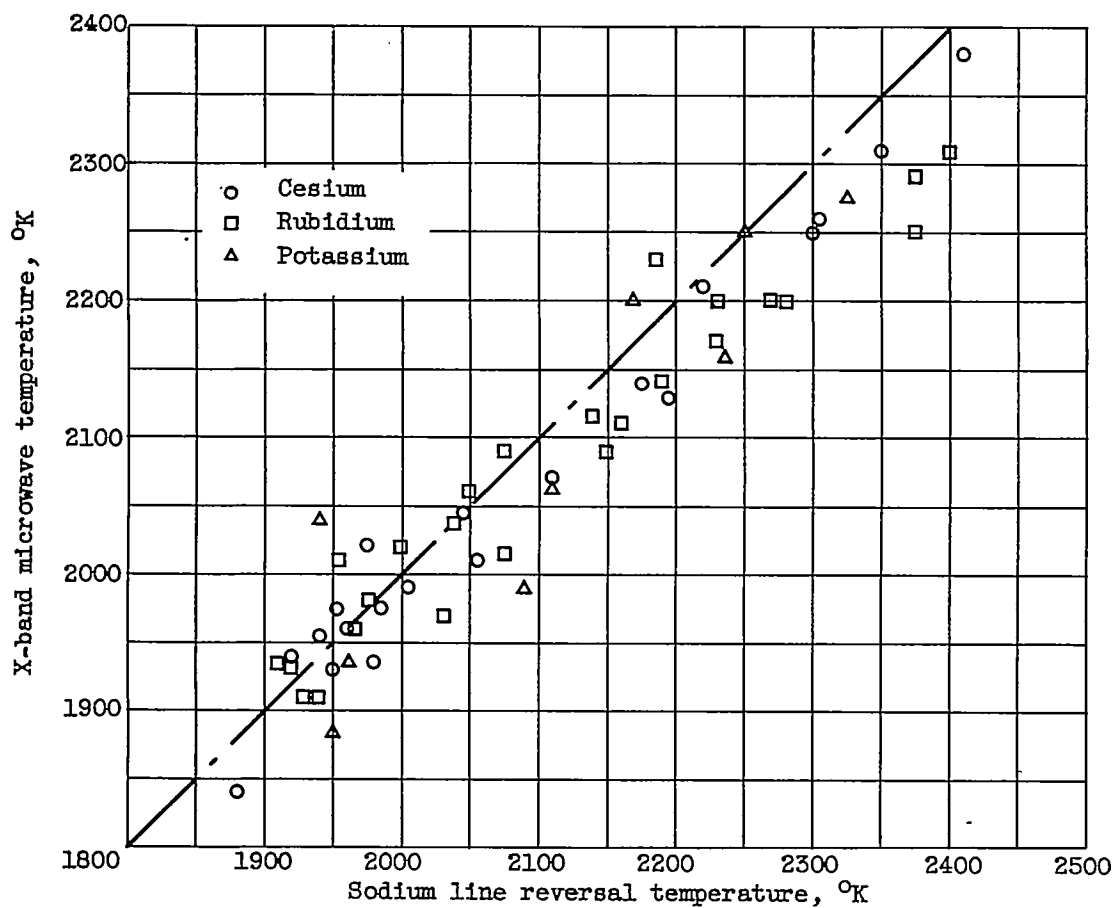


(b) K-band microwaves, obtained for accepted value of ionization potential of sodium (5.12 ev).

Figure 12. - Continued. Microwave temperature against sodium line reversal temperature for blast burner.

3109

CV-6 back



(c) X-band microwaves, obtained for experimental ionization potentials for cesium, rubidium, and potassium.

Figure 12. - Concluded. Microwave temperature against sodium line reversal temperature for blast burner.

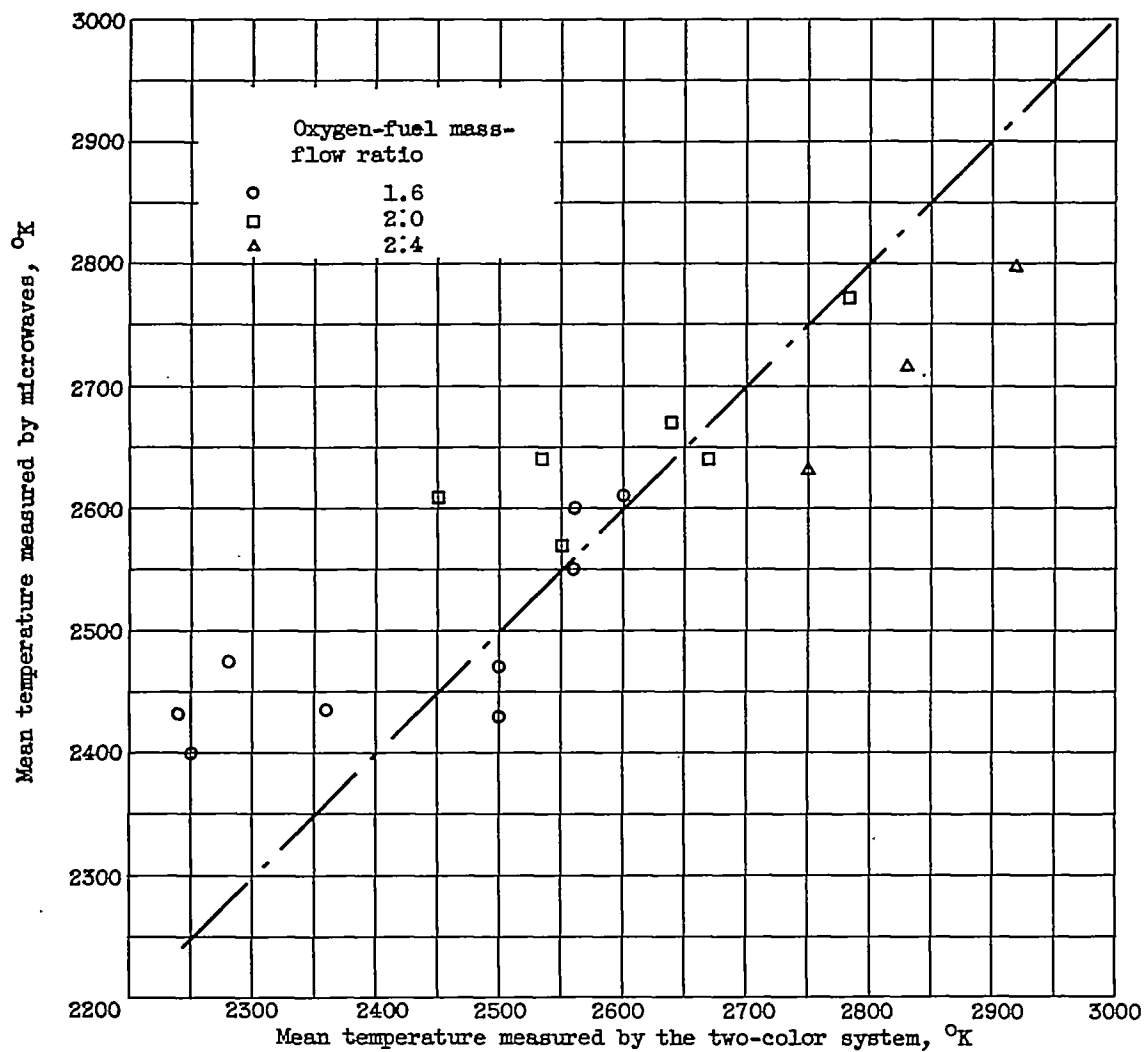
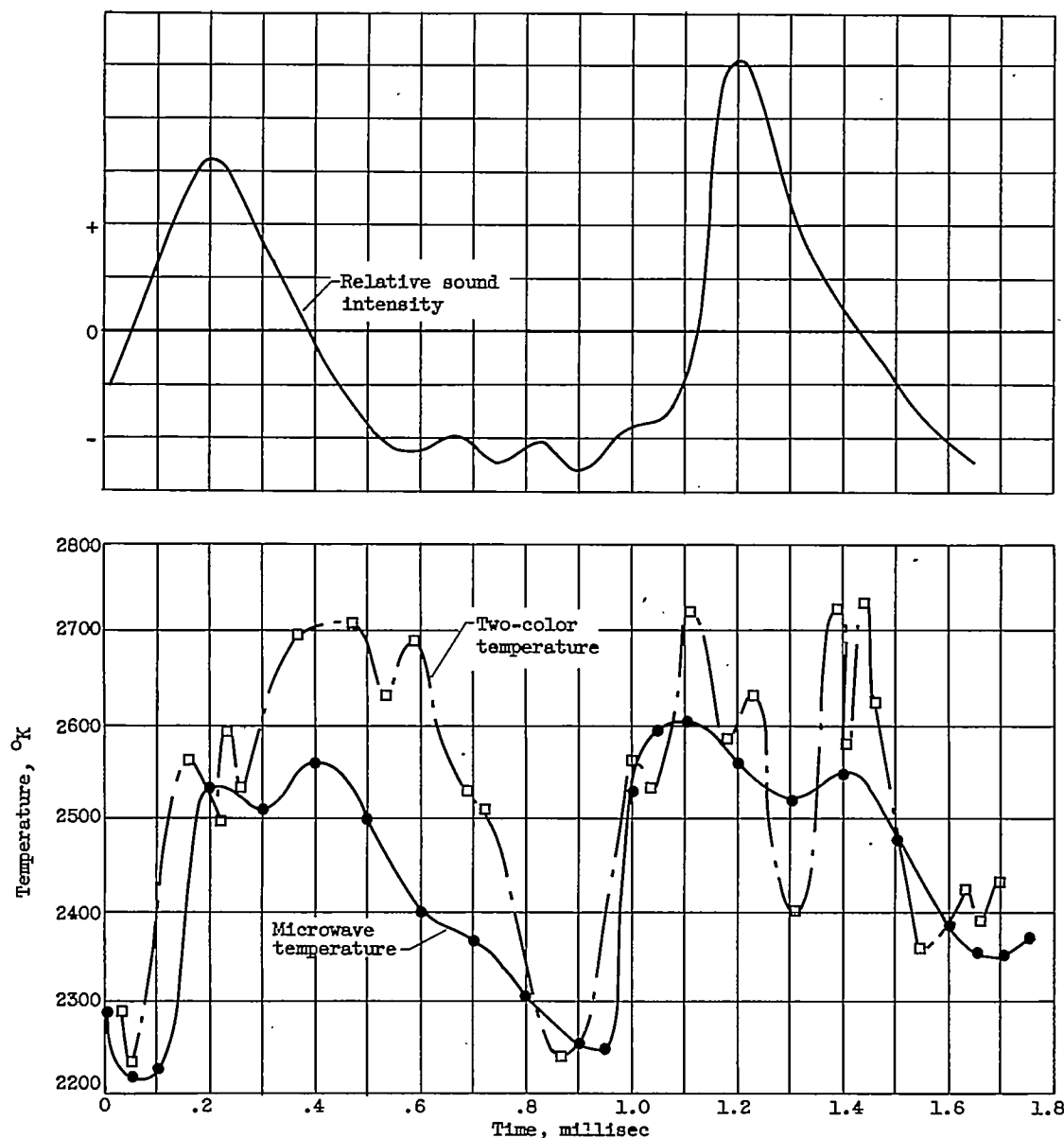


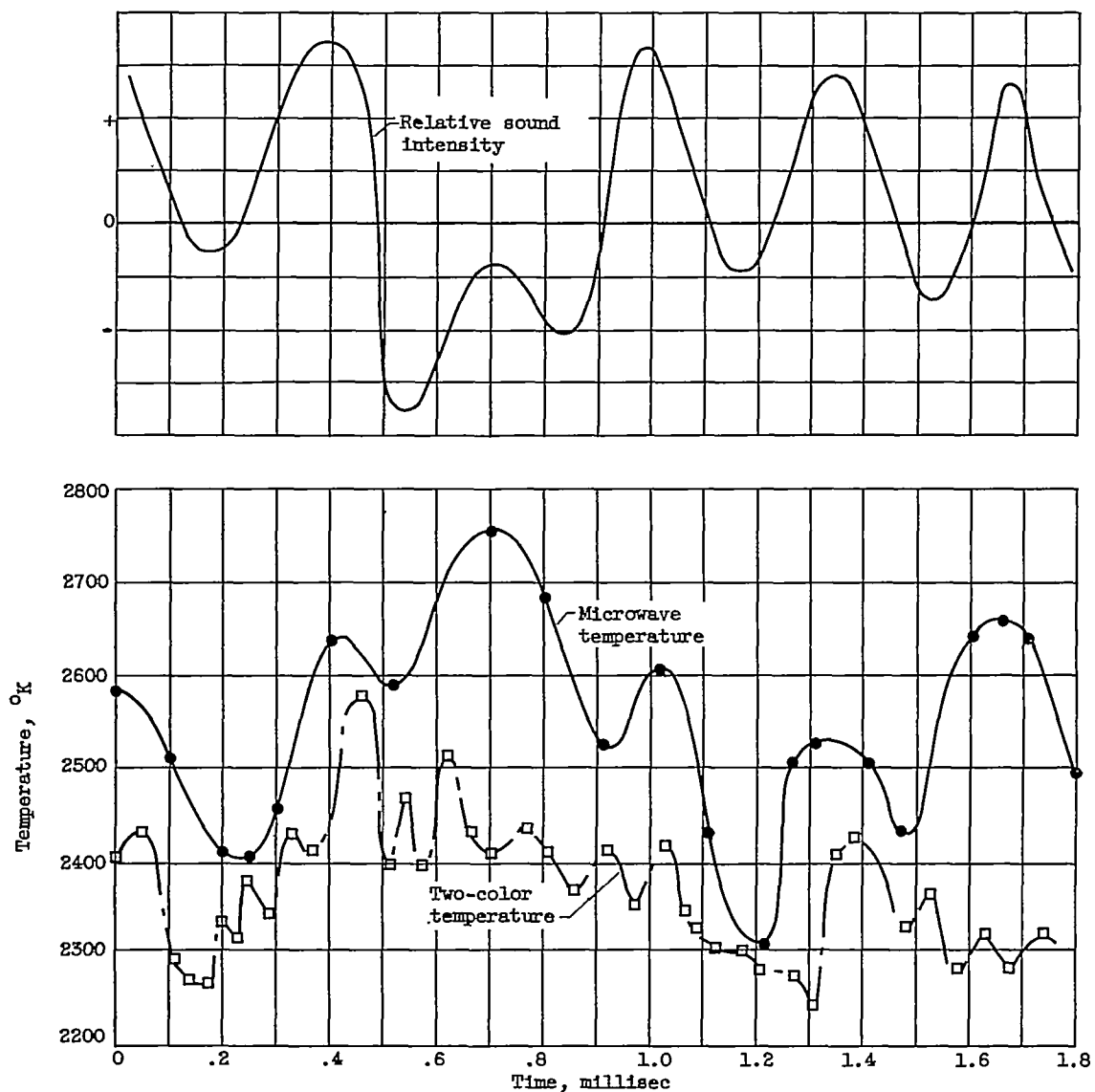
Figure 13. - Comparison of mean temperatures found by two methods of measurement on oxygen-heptane burner for three oxygen-fuel mass-flow ratios.

3109



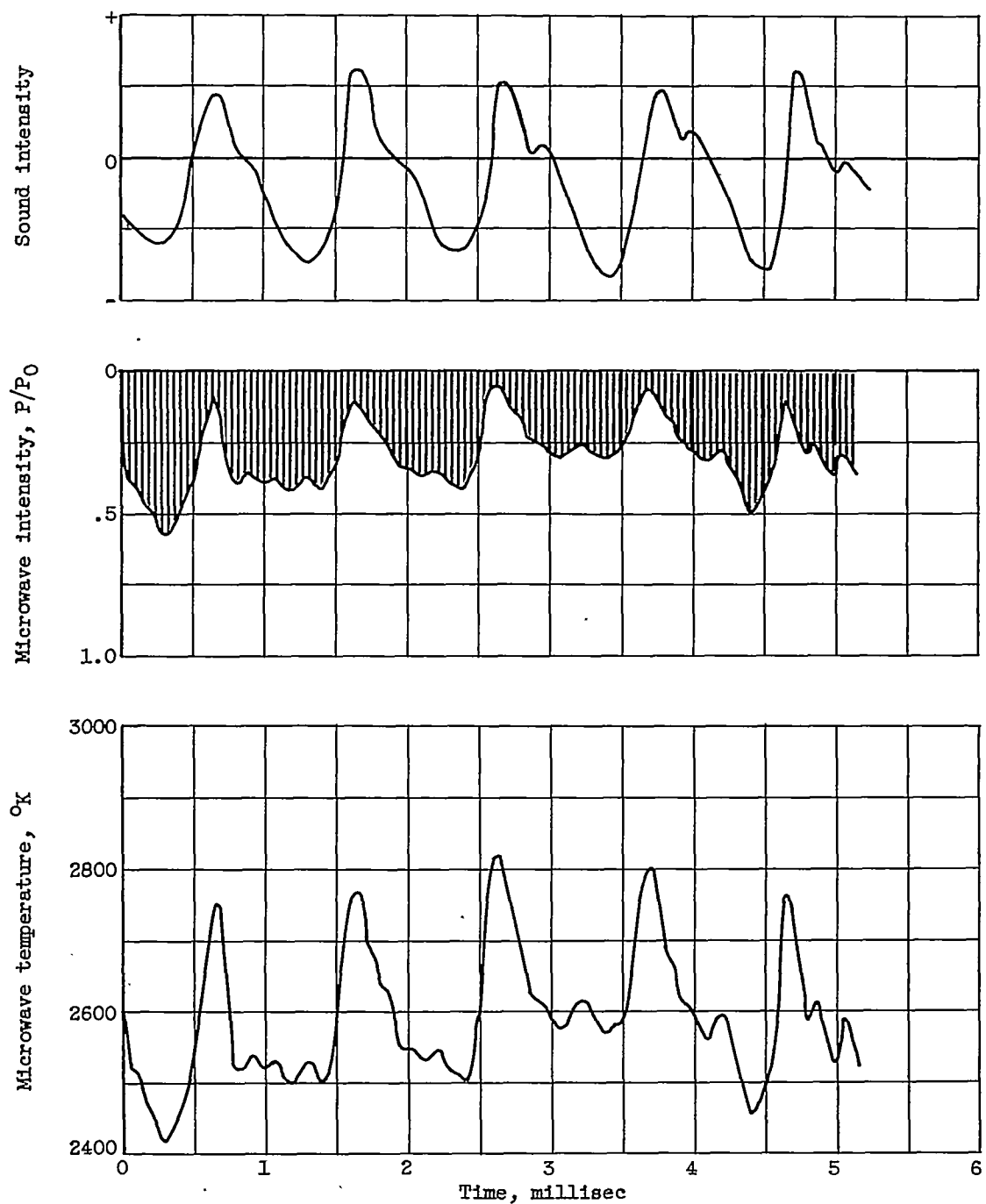
(a) Screaming at approximately 1000 cycles per second.

Figure 14. - Typical temperature variations in liquid propellant burner.



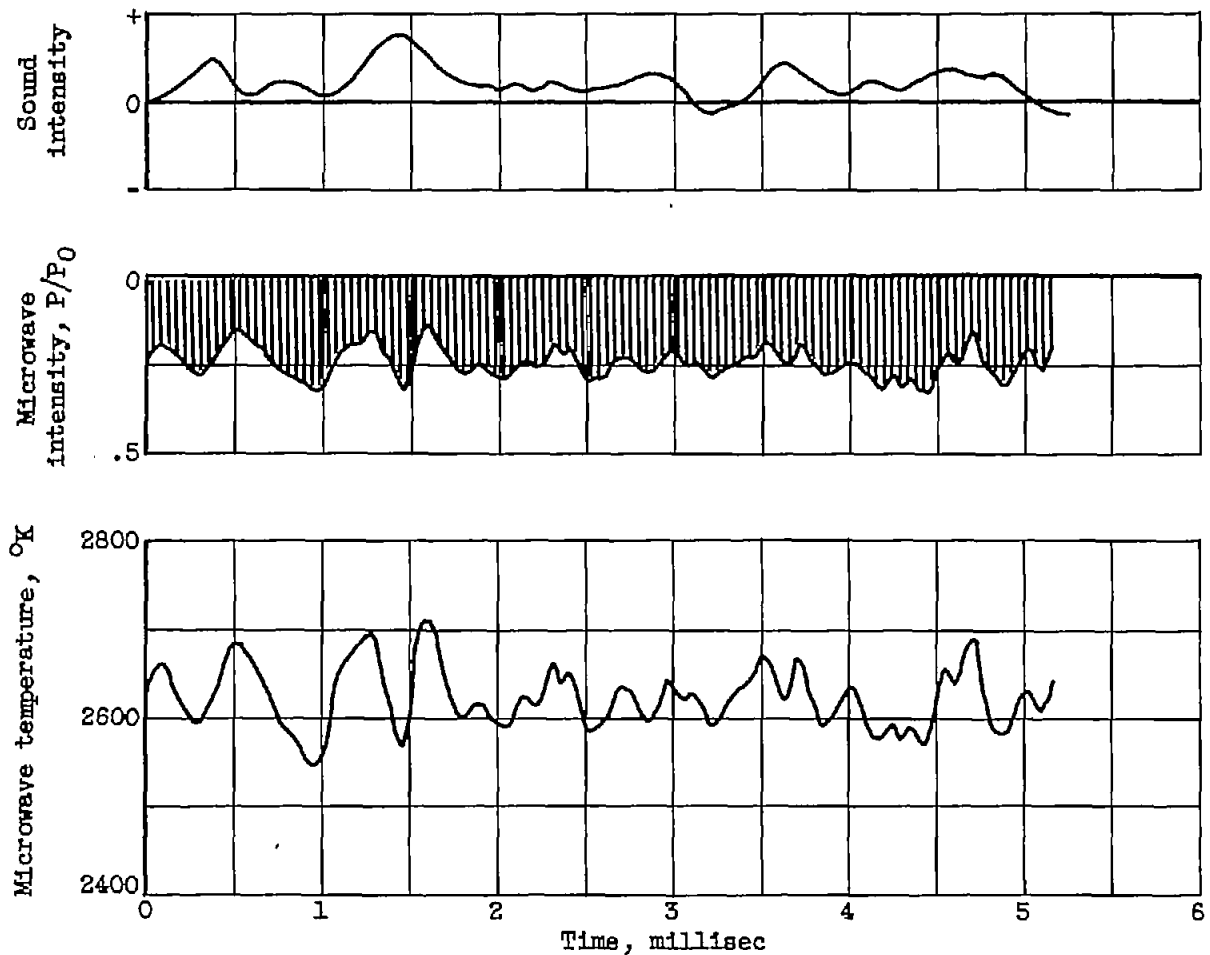
(b) Screaming at approximately 3000 cycles per second.

Figure 14. - Concluded. Typical temperature variations in liquid propellant burner.



(a) Screaming at 1000 cycles per second.

Figure 15. - Sound and microwave recordings of liquid propellant burner flame.



(b) Nonscreaming operation.

Figure 15. - Concluded. Sound and microwave recordings of liquid propellant burner flame.